BRNO UNIVERSITY OF TECHNOLOGY
VYSOKÉ UČENÍ TECHNICKÉ V BRNĚ

FACULTY OF CHEMISTRY
FAKULTA CHEMICKÁ

INSTITUTE OF MATERIALS SCIENCE
ÚSTAV CHEMIE MATERIÁLŮ

OPTIMIZATION OF METHODS FOR PROTEIN ANALYSIS RELEASED FROM THERMOSENSITIVE HYDROGEL

OPTIMALIZACE METOD PRO ANALÝZU PROTEINŮ UVOLNĚNÝCH Z TERMOCITLIVÉHO HYDROGELU

MASTER'S THESIS
DIPLOMOVÁ PRÁCE

AUTHOR — **Bc. Klára Lysáková**
AUTOR PRÁCE

SUPERVISOR — **doc. Ing. Lucy Vojtová, Ph.D.**
VEDOUCÍ PRÁCE

BRNO 2019

VYSOKÉ UČENÍ TECHNICKÉ V BRNĚ
FAKULTA CHEMICKÁ

Zadání diplomové práce

Číslo práce:	FCH-DIP1343/2018	Akademický rok:	2018/19
Ústav:	Ústav chemie materiálů		
Studentka:	**Bc. Klára Lysáková**		
Studijní program:	Chemie, technologie a vlastnosti materiálů		
Studijní obor:	Chemie, technologie a vlastnosti materiálů		
Vedoucí práce:	**doc. Ing. Lucy Vojtová, Ph.D.**		

Název diplomové práce:

Optimalizace metod pro analýzu proteinů uvolněných z termocitlivého hydrogelu

Zadání diplomové práce:

1) Literární rešerše o metodách využitelných k charakterizaci proteinů a o polymerních nosičových systémech zajišťujících kontolované uvolňování
2) Testování metod na modelových proteinech
3) Sledování vlivu chemických a fyzikálních parametrů na charakterizaci uvolněných proteinů
4) Aplikace vhodné metody na detekci růstových faktorů uvolněných z termocitlivého polymeru
5) Vyhodnocení
6) Závěr

Termín odevzdání diplomové práce: 10.5.2019:

Diplomová práce se odevzdává v děkanem stanoveném počtu exemplářů na sekretariát ústavu. Toto zadání je součástí diplomové práce.

Bc. Klára Lysáková student(ka)	doc. Ing. Lucy Vojtová, Ph.D. vedoucí práce	doc. Ing. František Šoukal, Ph.D. vedoucí ústavu

V Brně dne 31.1.2019

prof. Ing. Martin Weiter, Ph.D.
děkan

ABSTRACT

Proposed diploma thesis is focused on the release evaluation methods of both model proteins (albumin and lysozyme) and tissue healing protein (stable fibroblast growth factor 2; FGF2-stab) from the "smart" hydrogel carrier based on the biodegradable thermosensitive PLGA-PEG-PLGA triblock copolymer. In the theoretical part, a brief overview of thermosensitive polymers, their properties, structure and utilization of aforementioned proteins is described. Moreover, types of interactions that may occur between proteins and the polymeric carrier including drug release models are mentioned. In the experimental part, the structure of PLGA-PEG-PLGA triblock copolymer was characterized by the gel permeation chromatography and ^{1}H NMR while its visco-elastic properties including sol-gel transition were evaluated by the rheological analysis. Thesis goal was targeted to better understand the release of newly-patented FGF2-stab protein from injectable PLGA-PEG-PLGA hydrogel formed at physiological temperature. The amount of released FGF2-stab was measured by the UV-VIS spectrophotometer in the presence of a Bradford reagent that binds proteins resulting in shifting their absorption maxima from 280 nm to 595 nm. For the comparison, SDS-page electrophoresis, dividing protein by molecular weight, has been used. It has been find out, that model proteins, which were in different size but predominantly non-polar on their surface exhibited two-stage release dependent on both the diffusion and polymer degradation, whereas, FGF2-stab (25 $kg.mol^{-1}$) showed controlled one-stage first-order release from the PLGA-PEG-PLGA hydrogel forced only by diffusion, since it is predominantly a polar molecule located probably at the hydrogel micelle surface and not in their core. These results are very important to tune the protein release from hydrogel carriers to meet their certain application, in this case specifically in controlled tissue regeneration.

KEY WORDS

Drug delivery carriers, PLGA-PEG-PLGA copolymer, stable Fibroblast growth factor 2, Lysozyme, Albumin, protein release

ABSTRAKT

Předložená diplomová práce je zaměřena na metody hodnocení modelových proteinů (albuminu a lysozymu) a tkáňového léčivého proteinu (stabilního fibroblastového růstového faktoru 2; FGF2-stab) z „inteligentního“ hydrogelového nosiče na bázi biologicky odbouratelného termosenzitivního PLGA-PEG-PLGA triblokového kopolymeru. V teoretické části je zpracován stručný přehled termocitlivých polymerů, jejich vlastnosti, struktura a využití výše uvedených proteinů. Dále jsou zmíněny typy interakcí, které mohou nastat mezi proteiny a polymerními nosiči. V experimentální části byla struktura blokového PLGA-PEG-PLGA kopolymeru charakterizována gelovou permeační chromatografií a ^{1}H NMR, zatímco jeho viskoelastické vlastnosti včetně sol-gel přechodu byly hodnoceny reologickou analýzou. Hlavním cílem práce bylo lepší pochopení uvolňování nově patentovaného FGF2-stab proteinu z injektovatelného PLGA-PEG-PLGA hydrogelu tvořícího při gel při fyziologické teplotě. Množství uvolněného FGF2-stab bylo měřeno UV-VIS spektrofotometrem v přítomnosti Bradfordova činidla, které se váže na proteiny, což vede k posunu jejich absorpčních maxim z 280 nm na 595nm. Pro srovnání byla použita SDS-page elektroforéza, dělící protein podle molekulové hmotnosti. Bylo zjištěno, že modelové proteiny, které byly různé velikosti, ale převážně nepolární povahy, vykazovaly dvoustupňové uvolňování, zatímco FGF2-stab (25 kg.mol^{-1}) vykazoval z PLGA-PEG-PLGA hydrogelu řízené jednostupňové uvolňování, které probíhalo pouhou difúzí, jelikož se jedná převážně o polární molekulu, která se nachází pravděpodobně na povrchu micel, a ne v jejich jádru. Tyto výsledky jsou velmi důležité pro vyladění uvolňování proteinů z hydrogelových nosičů tak, aby vyhovovaly určité aplikaci, v tomto případě řízené regeneraci tkání.

KLÍČOVÁ SLOVA

Nosiče pro dodávání léčiv, PLGA-PEG-PLGA kopolymer, stabilní fibroblastový růstový faktor 2 (FGF2-stab), Lysozym, Albumin, uvolňování proteinů

LYSÁKOVÁ, Klára. *Optimization of methods for protein analysis released from thermosensitive hydrogel* [online]. Brno, 2019 [cit. 2019-05-06]. Available from: https://www.vutbr.cz/studenti/zav-prace/detail/117344. Diploma thesis. Brno University of Technology, Faculty of Chemistry. Supervisor Lucy Vojtová.

DECLARATION

I declare that the diploma thesis has been worked out by myself and that all the quotations from the used literary sources are accurate and complete. The content of the diploma thesis is the property of the Faculty of Chemistry of Brno University of Technology and all commercial uses are allowed only if approved by both the supervisor and the dean of the Faculty of Chemistry, BUT.

…….

student´s signature

Acknowledgement

I would like to thank my supervisor doc. Ing. Lucy Vojtová, Ph.D. for the willingness, valuable advice and time she has given to me. I also thank Nikola Ptáčková, Ph.D. and Ing. Markéta Zámečníková for their willingness in consultations. A next thanks go to Ing. Jana Brtníková, Ph.D. for GPC measurements and Ing. Kristýna Valová with help in rheological measurement.

Last but not least, I would like to thank my family for their support during my studies.

TABLE OF CONTENT

1 INTRODUCTION

Controlled drug delivery systems have several advantages over traditional drug forms. A reduction in the frequency and accurate amount of administered drug can be achieved. This leads to a reduction in the number of undesirable effects, to greater patient comfort and also to a reduction in drug consumption and thus a reduction in the environmental burden [28], [29].

The main study group as drug carriers are "smart" polymers. It is a type of polymer that reacts to any stimulus by changing properties. The most frequently used stimuli are changes in temperature, pH, light, ionic strength, mechanical stress, magnetic or electric field. Polymers studied as drug delivery vehicles must be non-toxic, biocompatible, and preferably biodegradable, or their degradation products must be so small that they can pass through the kidneys. The most commonly used temperature sensitive polymers are such as poly(N-isopropyl acrylamide), poly(N-vinyl acrylamide), poly(N-vinyl pyridine), pluronics® (poly(ethylene oxide)-*b*-poly(propylene oxide)-*b*-poly(ethylene oxide) triblock copolymers) and block copolymers based on the hydrophilic poly(ethylene glycol) (PEG) and hydrophobic poly(lactic acid) (PLA), poly(glycolic acid) (PGA) or poly(ε-caprolactone) (PCL). In this work, amphiphilic poly(lactic-*co*-glycolic acid)-*b*-poly(ethylene glycol)-*b*-poly(lactic-*co*-glycolic acid) (PLGA-PEG-PLGA) triblock copolymer was used as the biodegradable water-soluble copolymer that undergoes to a gel at physiological temperature. Along with increasing temperature in an aqueous environment, the PLGA-PEG-PLGA copolymer forms micelles having the hydrophobic core (PLGA) and the hydrophilic shell surface (PEG). Nowadays, drug carriers based on PLGA-PEG-PLGA copolymers are already commercially available under the names ReGel® and OncoGel® releasing under the controlled manner either hydrophobic drug paclitaxel (for cancer treatment) or hydrophilic hormone insulin (for diabetes treatment), respectively [23]-[32].

In the proposed diploma thesis, stable Fibroblast factor 2 (FGF2-stab), developed by the Enantis company (Brno, Czech Republic), was used as an protein-based drug, which stimulate the growth and the development of new vessels (angiogenesis), leading to improved wound healing and tissue development and contributing to the pathogenesis of several diseases (cancer or atherosclerosis). Other members of the FGF family have the potential for the use in tissue engineering, for example, FGF18 is believed to be a product to restore cartilage tissues [11].

The aim of this work is to ensure reproducible measurement of the FGF2-stab released amount from the thermosensitive, short half-live time PLGA-PEG-PLGA hydrogel and to determine the protein-hydrogel interactions in order to tune the protein release into a controlled way for medical applications.

2 THEORETICAL PART

2.1 Hydrogels for drug delivery

Hydrogels are three-dimensional, cross-linked networks of water-soluble polymers. Hydrogels can be made from virtually any water-soluble polymer, encompassing a wide range of chemical compositions and bulk physical properties. Furthermore, hydrogels can be formulated in a variety of physical forms, including slabs, microparticles, nanoparticles, coatings, and films [17].

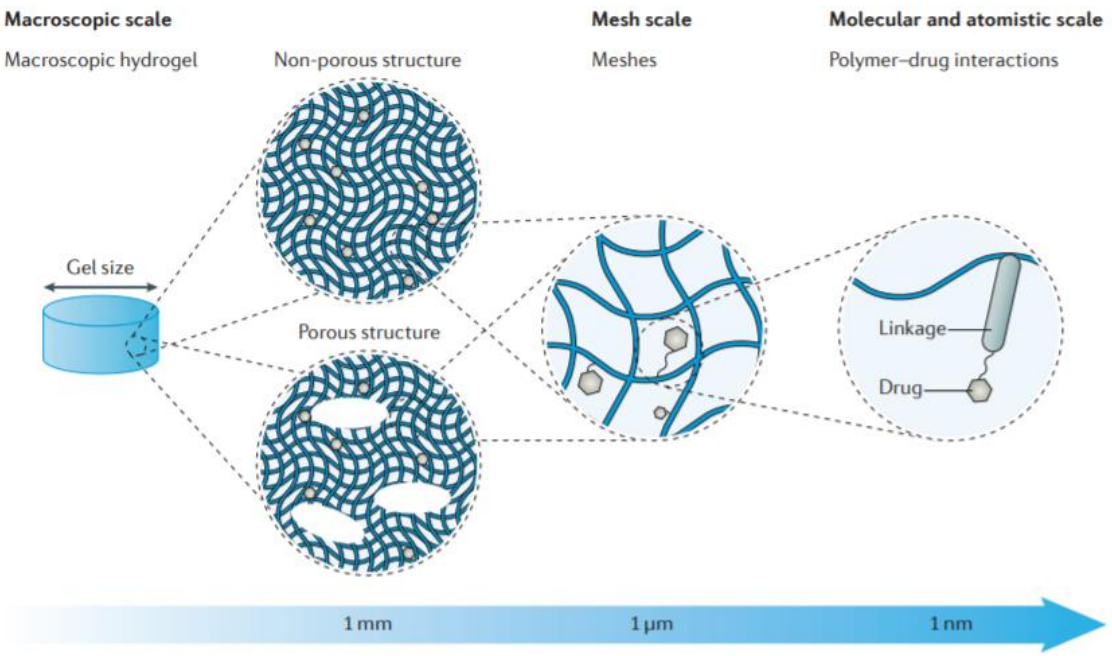

Fig. 1: The macroscopic design of hydrogels includes the size and porous structure. Hydrogels can be either non-porous or contain macroscopic pores that are 10–500µm in size. The spacing between polymer molecules in the network (that is, the mesh size) is tunable from around 5 to around 100nm. At the molecular (or atomistic) scale, drugs can interact with polymer chains via and range of mechanisms; shown here is a covalent linkage to a polymer chain [18].

In practice, hydrogels are used in experimental medicine in tissue engineering, oncology, immunology, regenerative medicine, cellular immobilization, separation of biomolecules or cells, and barrier materials to regulate biological adhesions. The unique physical properties of hydrogels have sparked interest in their use in drug delivery applications. Their highly porous (Fig. 1**Chyba! Nenalezen zdroj odkazů.**) structure can easily be tuned by controlling the density of cross-links in the gel matrix and the affinity of the hydrogels for the aqueous environment in which they are swollen. Their porosity ensures the loading of drugs into the gel matrix and the release depending on the rate of diffusion coefficient of the molecule through the gel network. The main benefits of hydrogels are pharmacokinetic, where the hydrogel-encapsulated drug is introduced into the site and provides a local drug concentration by slow release [17], [18].

Hydrogels are generally highly biocompatible and therefore widely used in in vivo sites. Biocompatibility is promoted by high water content (70 – 99 %) of hydrogels and the physiochemical similarity of hydrogels to the native extracellular matrix, both compositionally (particularly in the case of carbohydrate-based hydrogels) and mechanically. Hydrogels can be delivered to the body in various ways by surgical implantation, injection needle, or intravenous infusion, depending on the mode of use. The release method is also very important. It depends on the release time (short, long term) and release profile (continuous, pulsed). The degradation of the hydrogel occurs either during the release of the drug or after the release of all the amount. Biodegradability or dissolution may be designed into hydrogels via enzymatic, hydrolytic, or environmental (e.g. pH, light, temperature, magnetic or electric field) pathways; however, degradation is not always desirable depending on the time scale and location of the drug delivery device. The disadvantages of polymers include low tensile strength. Furthermore, high water content and large pore sizes lead to rapid drug release [17].

2.2 Polymers for drug delivery

The main reason for using polymers as carriers of biological drugs is often short half-lives, physical and chemical instability. Physical instability is an undesirable change in the highly ordered protein structure, resulting in denaturation, aggregation and precipitation. Chemical instability includes reactions such as oxidation, deamination, hydrolysis, and racemization. This problem is solved using polymers, which usually have better pharmacokinetics compared to small molecule drugs [28], [29].

The polymer must meet specific properties to be used as a carrier. It must be non-toxic, water-soluble, non-immunogenic, and must keep its function until it is excreted or degraded in the body. If the polymer is non-degradable (e.g. poly (methyl methacrylates)) it should be so small that it passes through the kidneys and does not accumulate. In the case of a degradable polymer, its degradation products must also be non-toxic [28], [29].

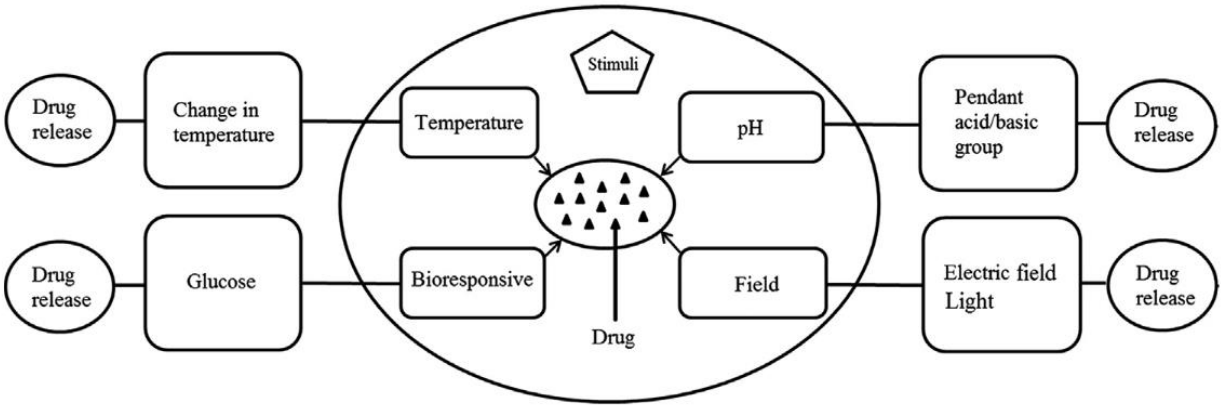

Fig. 2 :Various stimuli for controlling drug release from inteligen polymer drug delivery systems [29].

"Smart" polymers are the main group studied for controlled drug delivery. The "smart" or the benefit of these polymers is, that can react on some stimulus (see Fig. 2), either pH, temperature, light, ionic strength, magnetic or electric field or mechanical stress, which can be

easily changed. The Tab. 1 shows the stimuli and basic types of polymers that respond to these stimuli, as well as advantages and disadvantages for the use in medical applications. For example, a change in conformation, solubility, hydrophilic/hydrophobic balance or release bioactive molecules dissolution/precipitation, degradation, change of hydration state, swelling/collapse and micellization are pointed. Specifically, this thesis is focused on thermosensitive polymers for drug delivery [28], [29]

Tab. 1: Stimuli and basic types of polymers and their advantages and disadvantages in medical applications [29]

Stimulus	Material	Advantage	Disadvantage
Temperature	Poly (N-isopropyl acrylamide) Pluronic PLGA-PEG-PLGA Poly(*N*-vinyl caprolactam)	Simple production	Injectability issues under application conditions Low mechanical strength Problems with thermolabile drug instability
pH	Poly(methacrylic acid) Poly(vinyl pyridine) Poly(vinyl imidazole)	Suitable for thermolabile substances	Lack of toxicity data Low mechanical strength
Light	Modified poly(acryl amide)	Exact control over stimulus	Low mechanical strength Inconsistent light response
Electric field	Sulfonated polystyrene Poly(thiophene) Poly(ethyl oxazoline)	Pulsatile release with changes in electric current	Surgical implantation required Difficult optimization of electric field size
Ultrasound	Poly(ethylene vinyl acetate)	Controlled protein release	Surgical implantation required

2.3 Thermosensitive polymers

Temperature sensitive polymers in aqueous solvent are the most studied group of polymers used for medical applications. These substances suddenly change their solubility in response to a change in temperature, which controls the release rate of the incorporated drug and maintains physicochemical stability and biological activity. Temperature-dependent sol-gel transitions near body temperature are utilized. A typical feature of thermo-sensitive polymers is the presence of hydrophobic groups (e.g. methyl, ethyl and propyl groups). Polymers that do not dissolve when the temperature rises have a low critical solution temperature (LCST) and on the other hand polymers that dissolve have an upper critical solution temperature (UCST). The corresponding hydrogels exhibit so-called lower gel transition temperature (LGTT) or upper gel transition temperature (UGTT) [28], [29].

LCST polymer systems are preferred for medical applications because UCST systems need to be heated to a higher temperature and biomolecules can be degraded and deactivated. The most commonly used LCST thermosensitive polymers include poly(N-isopropyl acrylamide), poly(N-diethyl acrylamide), poly(N-vinyl alkylamide), poly(N-vinyl caprolactam),

phosphazene derivatives, pluronics®, polysaccharide derivatives, chitosan and PLGA-PEG-PLGA triblock copolymers [28], [29], [30].

2.3.1 Poly (N-isopropyl acrylamide)

Poly (N-isopropyl acrylamide) (PNIPAAm, Fig. 3) is one of the most studied temperature-sensitive polymers. It has an LCST of about 33 °C in aqueous solution and becomes insoluble in water. At 27 °C, 5% PNIPAAm in phosphate buffered saline (PBS) occurs for turbidity and gradual gelation. At 45 °C, the gel precipitates, it means that the water is released from the gel. The use is limited due to cytotoxicity probably caused by quaternary ammonia loading, biodegradability and platelet activation ability [34].

PNIPAM copolymers have been mainly studied for oral delivery of calcitonin and insulin. The peptide or hormone is immobilized in polymeric beads, which remains stable while passing through the stomach. Then in the alkaline intestine the beads disintegrate, and the drug is released [35].

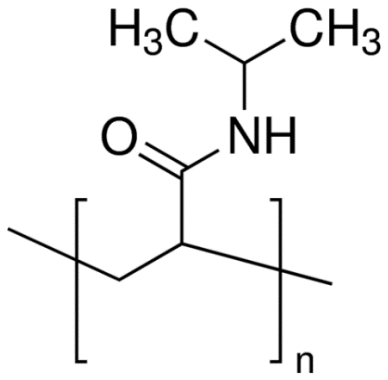

Fig. 3: Structure of poly (N-isopropyl acrylamide).

2.3.2 Poly(N-vinyl caprolactam)

In general, poly(N-vinyl caprolactam) (PNIPAAm) (see Fig. 4), resembles poly(N-isopropyl acrylamide) by being water-soluble, non-ionic, and LCST at about 32 °C in aqueous media. Unlike PNIPAAm, under acidic conditions, ammonia is not released, but rather carboxylic acid. LCST value may be modified by molecular weight, when increasing concentration and chain length decreases critical solution temperature (LCST). PNVCL is biocompatible and very stable to hydrolysis. Enzyme stability has been enhanced with PNVCL and has also been investigated as a release material in specific membranes and as a component of wound healing films [37].

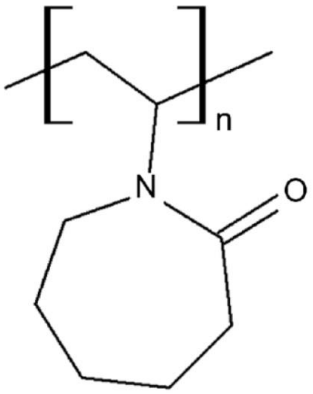

Fig. 4: Structure of poly (N-vinyl caprolactam).

2.3.3 Pluronic®

Pluronics® (also poloxamers see Fig. 5) are synthetic triblock copolymers of poly(ethylene oxide)-*b*-poly(propylene oxide)-*b*-poly(ethylene oxide) (PEO-PPO-PEO). It is an amphiphilic compound where poly(ethylene oxide) (PEO) is hydrophilic and poly(propylene oxide) (PPO) is hydrophobic. Amphiphilic molecules tend to form micelles, which are temperature dependent and affect the degradation properties of the biomaterial. Below the critical micelle temperature, both ethylene and propylene oxide blocks are hydrated, and the PPO block becomes soluble. This group of synthetic copolymers is thermo-reverse in aqueous solutions, and the sol-gel transition is governed by both molecular weight and concentration of each block of polymer [26], [27].

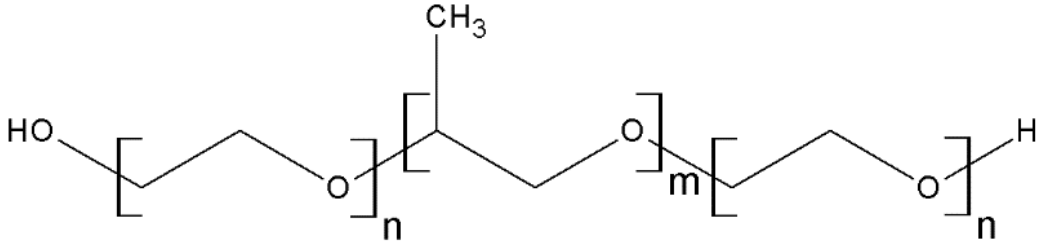

Fig. 5: Chemical structure of a poloxamer. It presents a central hydrophobic fragment of poly(oxy propylene) (PPO) and identical hydrophilic chains of poly(oxy ethylene) (PEO) at both sides [25].

Pluronic® F-127 (also Poloxamer 407) is used for tissue engineering due to commercial availability and sol-gel transition near physiological temperature and pH. The disadvantage is its rapid decomposition *in vivo* and therefore cross-linking with another α-hydroxy or amino acids is applied. Utilization was found as scaffold for hematopoietic stem cells and lung tissue because it inhibits surface-tissue adhesion. Pluronic F-127 also extends the effectiveness of painkillers (lidocaine) [26], [27]. Poloxamer 188 is used as a membrane sealant, *in vitro* studies of cardiac myocytes show signs of possible prevention of cardiomyopathy and heart failure in muscular dystrophy [27].

2.3.4 PEG/PCL Copolymers

These are amphiphilic copolymers consisting of blocks of hydrophilic poly(ethylene glycol) and hydrophobic poly(ε-caprolactone) (Fig. 6). PEG/PCL is a non-toxic, biodegradable

copolymer that is being investigated for the use in the targeted release of drugs for the treatment of cancer and thus to reduce systemic toxicity. It differs from PLGA-PEG copolymers in powder form. The PEG/PCL copolymer and drug are mixed above the melting point of PCL and the solution is allowed to gel for more than 24 hours at 4 °C. The limitation is in the high crystallinity and hydrophobicity of PCL, which prevents drug release [38].

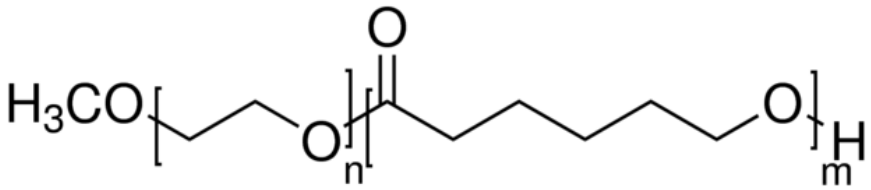

Fig. 6: Structure of PEG/PCL copolymers.

2.3.5 PLGA-PEG Copolymers

Polymer blocks based on the poly(lactic acid-*co*-glycolic acid) statistic copolymer (PLGA) and poly(ethylene glycol) (PEG) stand as (A) and (B), respectively, can be combined in different ratios to form AB, ABA and BAB type copolymers differing in sol-gel transitions parameters as well as hydrolytic stability. Subsequently, the work is focused mainly to the ABA triblock copolymer of poly(D,L-lactic acid-*co*-glycolic acid)-*b*-poly(ethylene glycol)-*b*-poly(D,L-lactic acid-*co*-glycolic acid) (see Fig. 7) mainly used for hydrophobic drug (paclitaxel) delivery due to its micellar structure in hydrogel, biocompatibility and controlled biodegradability. The triblock copolymer forms micelles in the aqueous medium where the non-ionic hydrophilic PEG forms the coating and thus affects the pharmacokinetics and biodistribution. On the other hand, the hydrophobic core (PLGA) can accommodate the hydrophobic drug [31], [32].

Since it is an amphiphilic block water-soluble copolymer, it undergoes a sol-gel transition by temperature change. By varying the ratio and the different molecular weights of the feedstock, copolymers can be prepared that will degrade for a different time and will undergo transition from sol to gel at different temperatures. Hydrogel formation cannot occur at high hydrophilic PEG content in copolymers, where PEG/PLGA > 0.56 [33].

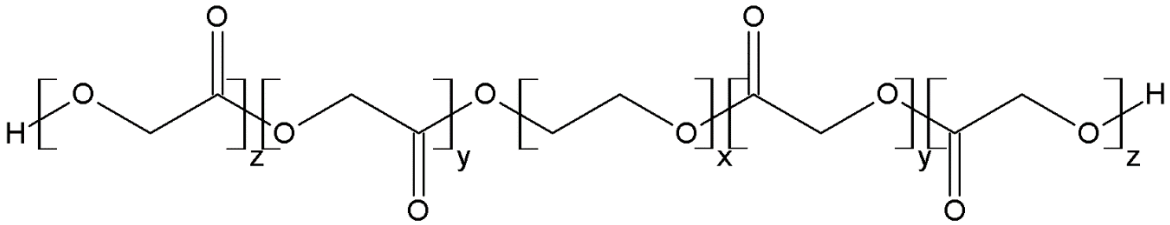

Fig. 7: Structure of triblock copolymer PLGA-PEG-PLGA [21].

2.3.5.1 ***ReGel*** ®

ReGel® is a triblock thermosensitive copolymer with a PLGA-PEG-PLGA framework. ReGel polymers transition from a free-flowing water-soluble low viscosity solution (sol-state) at temperatures between 2 and 15 °C to a viscous, water insoluble biodegradable controlled-

release gel (gel state) at body temperature. It is a water-insoluble gel that holds its integrity for over a month. It is therefore used for long-term release, where application is possible with a narrow-gauge needle. ReGel® is used to supply small hydrophobic molecules, peptides and proteins (insulin). Studies have shown that it is compatible with tissues at various anatomical sites [19], [20].

2.3.5.2 *OncoGel ®*

Paclitaxel, also known as Taxol®, is used to treat certain cancers, including ovarian, breast, lung, cervical, pancreatic, and Kaposi's sarcoma. It is an antineoplastic and antiangiogenic agent and a mitotic inhibitor. Its antitumor activity depends on concentration and time of exposure [19], [23].

ReGel® was used to deliver paclitaxel topically to tumours to avoid systemic toxicity associated with drug injection. OncoGel® is injected into the body, and gel formation occurs in response to body temperature, allowing for sustained release for up to 6 weeks [19], [23].

2.4 Polymers-drug interaction

Important properties in controlled drug release include information on how the drug and polymer interact. The power of interaction determines how much diffusion of the drug will slow down by diffusion. At high affinity, diffuse release can be completely stopped. This plays a major role in the delivery of small dosage forms that are smaller than the pore size of the polymer and hence a rapid initial release of high drug concentration occurs. This chapter describes the most common types of polymer-drug interactions [18].

2.4.1 Covalent conjugation

Covalent polymer-drug conjugates are special drug delivery systems where the drug or bioactive agent (peptides, proteins, growth factors, hormones, enzymes, etc.) is covalently bound to the macromolecular chain through a physiologically labile bond. The covalent bonds between the polymer and the drug can be of two types, highly stable or cleavable (see Fig. 8). Highly stable bonds stabilize the drug in the polymer (hydrogel) until the network degrades. However, cleavable covalent bonds are set to disintegrate after specific time, or in response to environmental stimuli. Thus, the drug is released at a programmed rate [18], [44].

High affinity bonds include amide bonds through carbodiimide chemistry, thiol bonds and other covalent bonds formed through metal-free click chemistry. Cleavable covalent linkages range from small-molecule linkages including ester bonds, disulphide bonds, and β-elimination cleavable linkages to macromolecular linkages like peptide sequences [18].

2.4.2 Electrostatic interaction

Electrostatic interactions are bonds between two oppositely charged molecules (see Fig. 8) and serve to create strong affinity between drugs and polymer chains in drug delivery systems. Since it is a non-specific charge-based interaction, attendance may be for controlled and simultaneous administration of multiple drugs from a single system. Drug release occurs either by matrix degradation or when electrostatic inertia is detected by mobile ions from

the environment. These interactions are used, for example, in alginate hydrogels that carry negative charges to deliver heparin-binding cationic growth factors (such as VEGF) that serve to promote tissue regeneration [18], [45].

If there is no formation of electrostatic interactions between the polymer and the drug, or the interactions are not strong enough, the third component (agent) can be used. Heparin, for example, has been incorporated into hydrogels to control heparin-binding proteins such as VEGF and basic fibroblast growth factor (bFGF). For example, the sulfonate groups are used to increase the electrostatic interactions between alginate hydrogels and protein drugs to increase release time[17], [18].

2.4.3 Hydrophobic interaction

The term hydrophobicity is a repulsion between a non-polar compound and a polar environment such as water. In biological systems, hydrophobic interactions are of great importance in protein folding and stabilization of their structure. The use of hydrogels as carriers of hydrophobic drugs is problematic because of the high-water content and hence their hydrophilic nature. The phase separation between the encapsulated hydrophobic drugs and the hydrogel can lead to a reduction in the strength and stability of the hydrogel. This problem is solved by linking hydrophobic domains or binding sites for hydrophobic drugs (see Fig. 8) [18], [46].

One possibility is to copolymerize hydrophilic and hydrophobic monomers (e.g. PLGA-PEG-PLGA), where the hydrophobic molecule (e.g. cyclodextrin and cholesterol) can be attached to the hydrophobic chain via hydrophobic interactions. Thiocholesterol has been incorporated into hydrogels of poly(vinyl alcohol) for delivery of hydrophobic drugs. However, by incorporating hydrophobic moieties, it can reduce the water content of hydrogels and potentially alter their biochemical and physical properties. To this end, the inclusion of cyclodextrins in hydrogels is advantageous because they do not alter the overall hydrophilicity of the hydrogels. These macrocyclic oligosaccharides contain both external hydrophilic character and internal hydrophobic pockets into which hydrophobic drugs can bind. In such systems, drug release is independent of hydrogel mesh size [17], [18], [46].

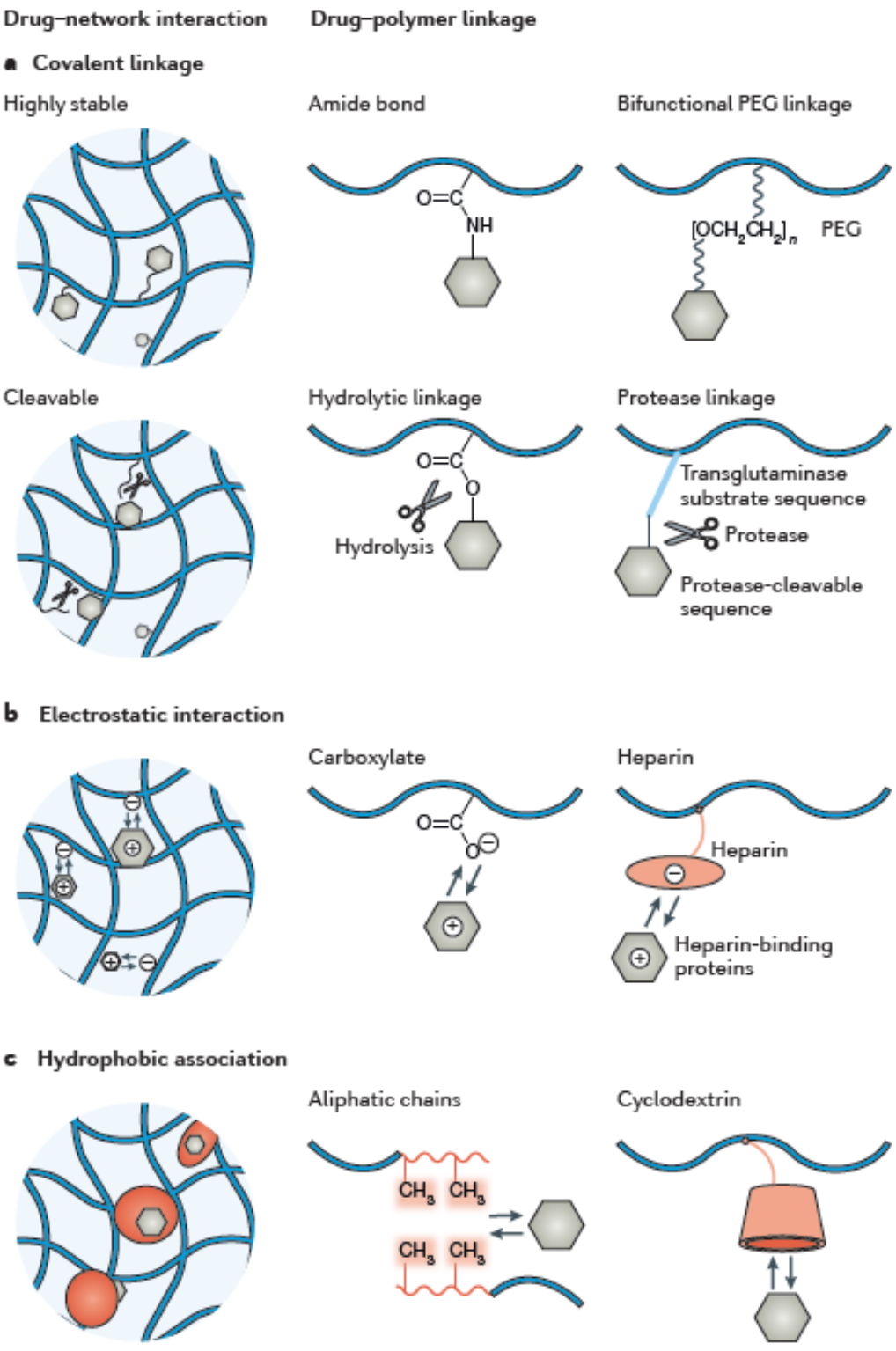

Fig. 8: Representative chemical interactions between a drug and polymer chains. a) Highly stable covalent linkages immobilize the drugs inside the hydrogel. Strategies include the formation of amide bonds and the use of long-chain poly(ethylene glycol) (PEG) linkages. b) Cleavable covalent linkages release the drug as a result of hydrolysis or the activity of enzymes like proteases. c) Electrostatic interactions between a charged drug and the polymer chain can slow release. This can be exploited using polymers carrying charges, such as carboxylate groups and those mimicking heparin-binding groups. d) Hydrophobic drugs associate with hydrophobic domains such as aliphatic chains and cyclodextrin [18].

2.5 Drugs release models

Controlled drug delivery technology has been extensively studied over the past six decades. The reason was associated with the problems that arose after the application of standard oral medications multiple times a day. For example, fluctuation (higher or lower) of the drug substance in the blood (than the therapeutic optimum) may result in escalation of adverse drug effects on one side and non-cure on the other side. In the following paragraphs, model examples for polymer drug release (see Fig. 9) will be described [43].

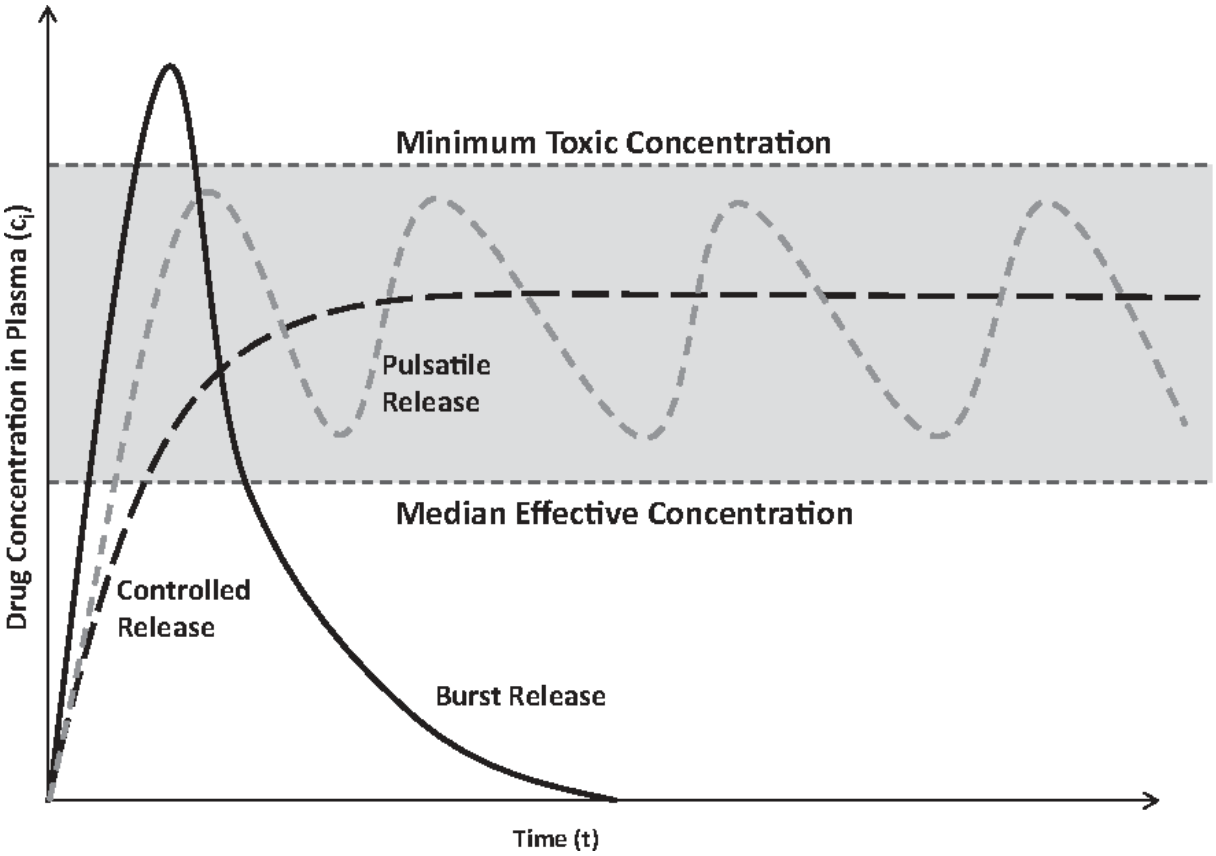

Fig. 9: Therapeutic band with showing impact of burst release, pulsatile release, and controlled release relative to effective concentration and toxic concentration [42].

Controlled release drug systems offer great advantages over conventional dosage forms. Benefits include topical drug delivery, reduced dosage frequency, diminished in vivo fluctuation of drug concentration and maintenance of drug concentration in the desired range, and an evaluation of side effects. Generally, controlled release dosage forms are designed to maintain constant concentrations of the drug in the blood, tissues, or target organs. First, the initial higher dose of drug is released from the system and the maintenance dose is released in a constant rate [42].

The term "burst release" refers to the release of a high amount of drug within a short time. This mode of release can be seen in two ways, negatively where local or systemic toxicity may occur due to high drug concentration and short in vivo disintegration time (rapid loss of activity),

hence more frequent dosing. Or from a positive point of view, when the drug is quickly delivered to the desired location [41].

Pulsed or pulsatile drug release provides intermittent action, the drug is released in portions at abruptly defined intervals. This type of release is found in the human body, namely the release of hormones (daily fluctuations). For this mode of delivery, it is assumed that the constant plasma drug levels are not preferred and are the optimal therapeutic effect coming from the periodically fluctuating drug concentration. A typical example is the insulin hormone, when pulse release occurs after food intake, and blood glucose levels are controlled. Furthermore, gastrointestinal hormones also show pulsatile release due to the presence of sweat in the gastrointestinal tract. And lastly, the menstrual cycle is controlled by pulsed release of hormones such as estrogen and progesterone [40].

A large number of biological functions in the body are regulated by time and pulse release, so it may be necessary to deliver drugs in this way. A continuous dose of hormones generally induces down regulation of hormone receptors on target cellular membranes and shows undesired effects in the body [40].

2.6 Proteins

Proteins are biomacromolecular substances whose proportion in tissues of higher organisms and humans exceeds 80%. They consist of at least 100 L-α-amino acids bound together into polypeptide chains by peptide bond (see Fig. 10). The order and number of amino acid residues in the chain are specific for each protein. Like polysaccharides or nucleic acids, proteins are involved in cell processes. Proteins have both structural and mechanical functions, which include actin and myosin in the muscles, as well as scaffolding in the cytoskeleton to maintain the shape of the cells. Many proteins catalyse biochemical reactions and are referred to as enzymes. Proteins are essential in the diet because they provide essential amino acids that cannot be synthesized [12].

According to the shape, proteins are distinguished into fibrillar, membrane and globular, although the boundaries between them are not clearly defined. Fibrillar or filamentous proteins occur in the cytoskeleton of cells. They are insoluble in water. Representatives are, for example, collagen or keratin. Membrane proteins are part of bio-membranes. It performs various functions, such as the transport of substances, the transmission of signals, or merely contributes to the strengthening of membranes. The last globular proteins are spherical, water soluble. Because it is a very large group, their biological functions are quite diverse. Examples include antibodies and enzymes [12].

However, proteins can also be divided chemically to which are composed of only amino acids, and compound containing a non-protein part. Compound proteins include hemoproteins where blood is a hem (e.g. hemoglobin), lipoproteins with a lipid moiety, nucleoproteins with nucleic acid, glycoproteins with carbohydrate, metalloproteins with metal cations (e.g. ferritin), and phosphoproteins with phosphoric acid residues [13].

The next chapters will describe the structure, properties and utilization of both the model proteins (lysozyme and albumin) and wound-healing protein (FGF2-stab) studied in this thesis.

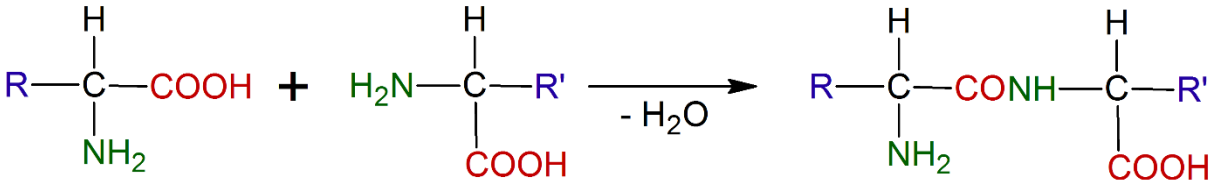

Fig. 10 : Scheme of polypeptide chain formation.

2.7 Lysozyme

Lysozyme is an antibacterial enzyme found in saliva, tears, egg white, nasal mucus, blood plasma and breast milk. Another name is N-acetylmuramidglycan hydrolase and belongs to the hydrolase group. The common feature of all lysozymes is their ability to hydrolyse the β-(1,4)-glycosidic bond between alternating N-acetylmuramic acid (NAM) and N-acetylglucosamine (NAG) residues of peptidoglycan, and unique bacterial cell wall polymer. Three main types of lysozyme-c-type (chicken-HEWL or conventional type), g-type (goose-GEWL) and lysozyme type i (invertebrate type) have been identified in the animal kingdom [13], [14], [15].

2.7.1 Structure

Hen's lysozyme (HEWL) is most closely described (see Fig. 11). HEWL catalyses the hydrolysis of its substrate so efficiently that it proceeds up to 10^{10} times faster than the non-catalysed reaction. The molecular weight of lysozyme is approximately 14.7 $kg.mol^{-1}$ and consists of 129 amino acid residues and is internally cross-linked by 4 disulphide bonds. It does not contain coenzymes or metal ions, so its three-dimensional structure, catalytic effect and specificity are determined solely by the order of amino acids [13].

The polypeptide chain has a relatively irregular secondary structure, contains several heliacal segments, as well as a three-stranded anti-parallel β-folded sheet that occupies most of the binding groove. Most non-polar chains are out of contact with the aqueous solvent within the molecule [13].

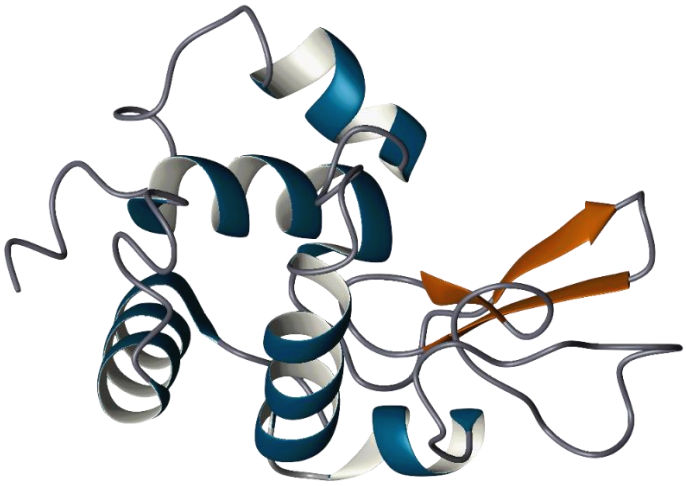

Fig. 11: Structure of lysozyme [13].

2.7.2 Property and Uses

The human lysozyme used in this thesis differs from the other species only in sequence, but not in its reaction mechanism.

The most prominent feature of the molecule is the pronounced groove, the binding site with six binding sub-sites (see Fig. 12) for substrates or inhibitors. The residues responsible for the cleavage of the bonds lie between D and E near the carboxyl groups of Asp 52 and Glu 35. The acetal bond of the substrate is likely to be protruded by Glu 35, while the negatively charged Asp 52 stabilizes the emerging carbonium ion from the opposite side [22].

Lysozyme has been shown to be effective against bacteria causing food-borne disease and spoilage at concentrations of 10 to 200 mg/L. Overall, it may be concluded that lysozyme can be active as an additive to foods containing susceptible bacteria and acts to lower the levels of the bacteria or inhibits their initial growth [16].

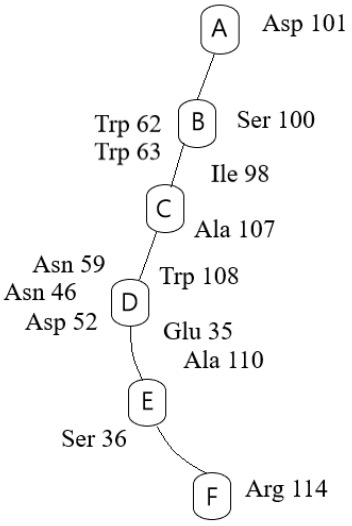

Fig. 12: Scheme of the catalytic site in the lysozyme slit. A to F are glycosidic units of hexasaccharide. For residues forming the slot region, the lysozyme sequence numbers are shown [22].

2.8 Albumin

Albumin is a specific and major protein of human and animal blood plasma (45 g/L). The source of albumin in the human body is the liver, which produces 10-15 g daily and its half-life in the body is 19 days on average [2].

Albumin is responsible for colloidal osmotic blood pressure in the human body, is essential for fat metabolism, can bind bilirubin, and many drugs are used to treat haemorrhagic shock and burns. Specifically, it binds Cu^{2+}, Ni^{2+} and non-specifically binds Ca^{2+} and Zn^{2+}, thereby securing the transport of these metal ions in the blood. In biochemistry, it is used as a solvent in ELISA tests [1], [2].

2.8.1 Structure

The molecular weight of albumin is 69 $kg.mol^{-1}$ and accounts for about 60% of total plasma proteins. Human albumin consists of one 585 amino acid polypeptide chain and contains 35 cysteine molecules, 17 disulphide bonds that stabilize the tertiary structure and one free cysteine molecule at position 34 with the thiol SH group making it capable of forming dimers [1], [2], [5].

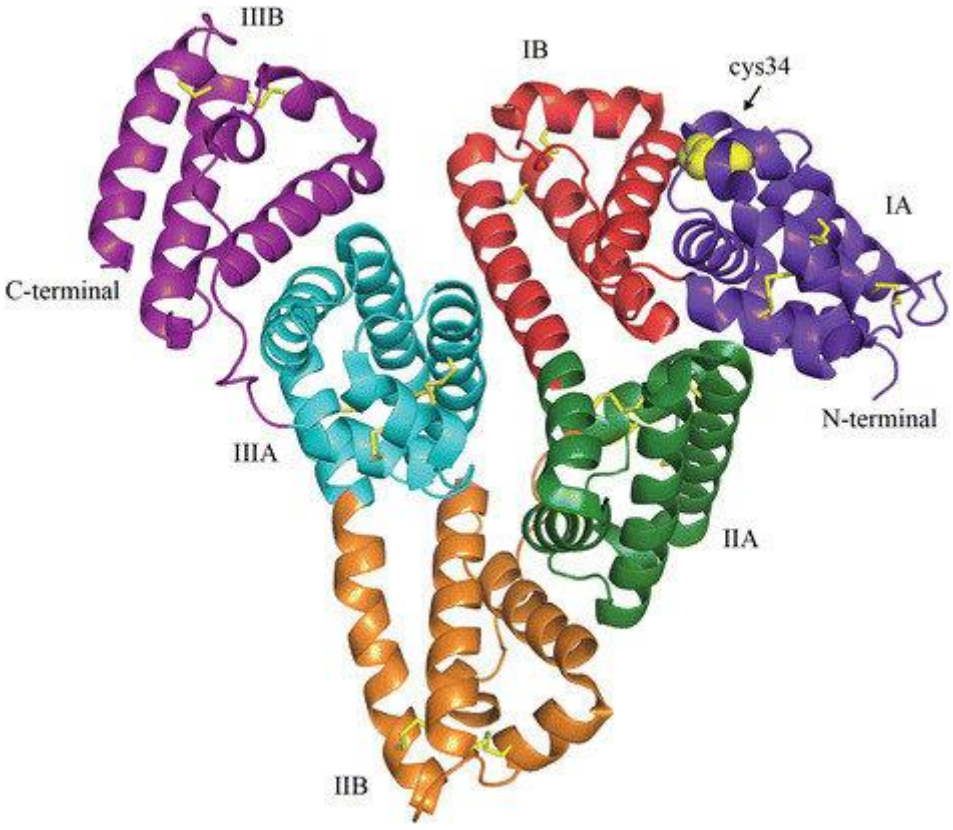

Fig. 13: Crystal structure of human serum albumin. The illustration shows the tertiary structure of human serum albumin in complex with stearic acid. The three domains of albumin are shown in purple (IA), red (IB), green (IIA), orange (IIB), blue (IIIA), and violet (IIIB). Yellow sticks depicture disulfide bridges, and yellow spheres highlight the available cysteine 34 in domain IA [2].

HSA is a globular, ellipsoidal and helical protein containing many flexible strands in its structure, and the molecule is heart shaped (see Fig. 13). The HSA molecule is divided into three domains and each domain contains two subdomains (A and B) formed by 4 (subdomain A) or 6 (subdomain B) by helical structures. The last helix of one domain is always linked to the first helix of the following domain and hence the HSA molecule consists of a total of 28 helical structures. Albumin contains two stable binding sites capable of binding most drugs at therapeutic concentrations. According to the Sudlow nomenclature, bulky heterocyclic anions (bilirubin, anticoagulants, non-steroidal anti-inflammatory drugs) bind to Sudlow site I (located in subdomain IIa) while Sudlow's site II (located at IIIa) is preferred by aromatic carboxylates ketoprofen or benzodiazepines such as diazepam) [3].

2.8.2 Properties and Uses

Albumin is an acidic and highly aqueous protein. This property originates in the primary structure and its high total charge (approximately 185 ionized groups per molecule at pH 7.0). It is stable at pH 4 – 9, soluble in 40% ethanol and can be heated to 60 °C for 10 hours without harmful effects [4].

Already in the mid-twentieth century, first studies emerged demonstrating the fact that tumours capture proteins from blood plasma and use their degradation products to rapidly multiply. Albumin distribution studies have shown that 3 – 25 % of the administered protein dose accumulates in the tumour. This makes albumin a promising drug carrier for, for example, targeted cancer treatment. Albumin nanoparticles attract attention because they have several unique properties over other proteins. Albumin is non-toxic to the body, capable of reversibly binding many hydrophobic drugs. Due to the large number of charged amino acid residues, it can electrostatically bind both positively and negatively charged substances while being able to covalently bond with the drug with the participation of carboxyl or amino groups. In addition, it has a very advantageous pharmacokinetic profile due to its half-life in the bloodstream (19 days) [4], [6].

2.9 Fibroblast growth factor (FGF)

Fibroblast growth factors (FGF) regulate a wide range of biological functions, including cell proliferation, inducing cellular homeostasis, promoting angiogenesis and wound healing. FGFs have multiple functions through binding and activation of fibroblast growth factor (FGFR) receptors and the main signal through FGFR stimulation is the RAS/MAP kinase pathway. FGF was discovered in pituitary extracts in 1973 (is widely expressed in cells and tissues). Acid FGF (FGF1) and basal (FGF2) were originally isolated from brain and pituitary as growth factor for fibroblasts. Since then, at least 22 different FGFs have been identified or isolated [9], [10][9].

FGFs have been found in both vertebrates and invertebrates. Many FGF genes have been identified in vertebrates, including ten FGFs in zebrafish (FGF2–4, 6, 8, 10, 17a, 17b, 18, 24), six in Xenopus (FGF2–4, 8–10), 13 in chickens (FGF1–4, 8–10, 12, 13, 16, 18–20), 22 in mice (FGF1–18, 20–23) and humans (FGF1–14, 16–23), whereas only three Drosophila FGF genes and two Caenorhabditis elegans FGF genes have been observed in invertebrates. Human FGFs contain 22 members: FGF1, FGF2, FGF3 (INT2), FGF4, FGF5, FGF6, FGF7 (KGF), FGF8

(AIGF), FGF9, FGF10, FGF11, FGF12, FGF13, FGF14, FGF16, FGF17, FGF18, FGF19, FGF20, FGF21, FGF22, and FGF23 [9].

By phylogenetic analysis, the human FGF family can be divided into seven subfamilies (see Fig. 14): FGF1, FGF4, FGF7, FGF8, FGF9, FGF11, and FGF19. Subfamily FGF1, FGF4, FGF7, FGF8, FGF9, FGF11 and FGF19 contain FGF1 and 2, FGF4, 5 and 6, FGF3, 7, 10 and 22, FGF8, 17 and 18, FGF9, 16 and 20, FGF11, 12, 13 and 14 and FGF19, 21 and 23. In contrast to phylogenetic analysis, gene localization analysis shows that the human FGF gene family can be divided into six subfamilies: FGF1 / 2/5, FGF3 / 4/6/19/21/23, FGF7 / 10/22, FGF8 / 17/18, FGF9 / 16/20 and FGF11 / 12/13/14. The members of FGF8, FGF9 and FGF11 subgroups are like those of FGF7 / 10/22, FGF8 / 17/18, FGF9 / 16/20 and FGF11 / 12/13/14 subfamilies in gene position analysis [9].

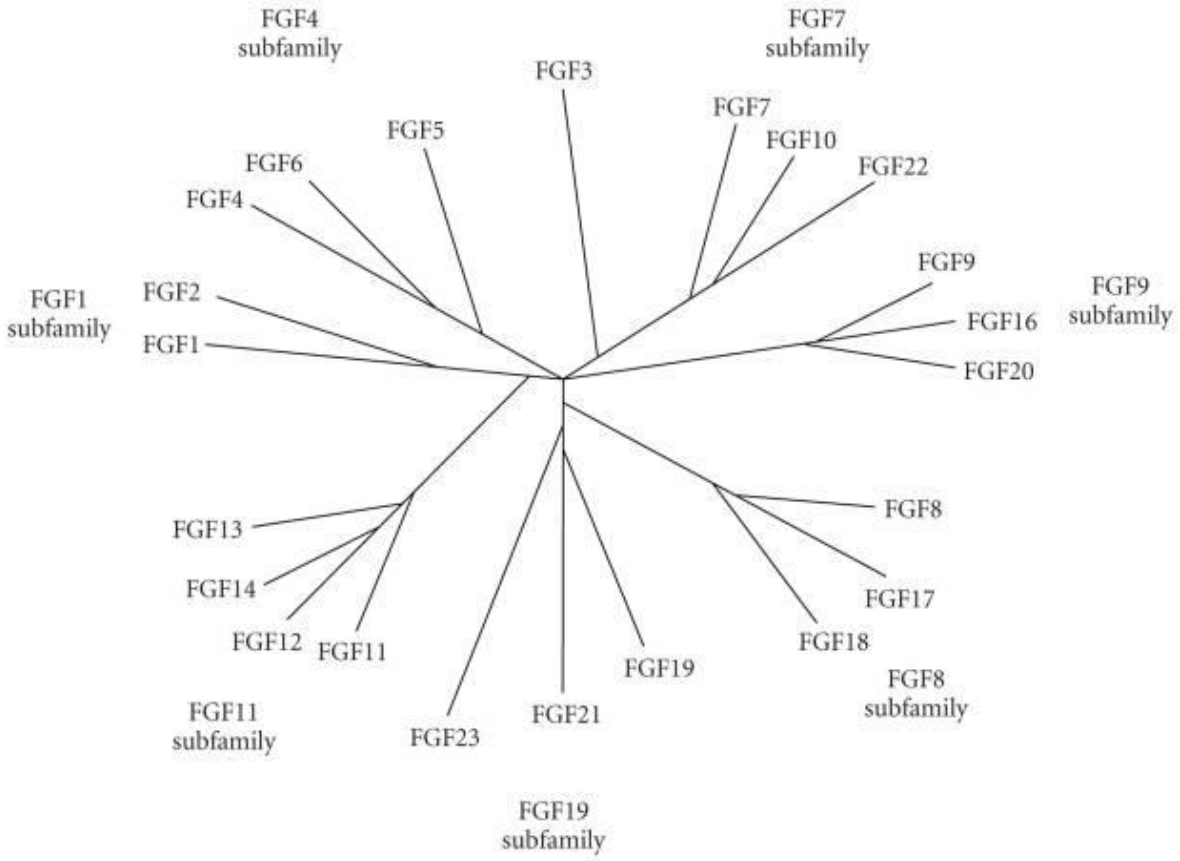

Fig. 14: Subfamily of fibroblast growth factor [9].

2.9.1 Structure and properties

The molecular weight of FGF in vertebrates ranges from 17 to 34 $kg.mol^{-1}$, while in invertebrates it is about 84 $kg.mol^{-1}$. All family members have a sequence of 120 amino acids that display 16 – 65 % sequence identity [9].

The physiological properties of FGF are due to FGFR binding. The FGF family of mammals is composed of 18 ligands that induce their action through four highly conserved transmembrane tyrosine kinase receptors (FGFR1, FGFR2, FGFR3 and FGFR4). Four FGFRs have been

identified in humans and mice and encode receptor tyrosine kinases (about 800 amino acids) that contain an extracellular ligand domain with three immunoglobulin domains (I, II and III), a transmembrane domain, and a cleaved intracellular domain of the tyrosine kinase domain. FGFRs are expressed on many different cell types and regulate key cellular behaviour, such as proliferation, differentiation and survival, which cause FGF signalling to be susceptible to subversion by cancer cells. Unlike other growth factors, FGF interacts with heparin or heparan sulfate with proteoglycan (HSPG) to activate FGFR and induce pleiotropic responses that lead to different cellular responses induced by this large family of growth factors [9].

2.9.2 Fibroblast growth factor 2 (FGF 2)

FGF 2 stimulates the growth and development of new vessels (angiogenesis), which contribute to the pathogenesis of several diseases (cancer, atherosclerosis), wound healing and tissue development. In addition to structural similarity between FGF-2 and other FGF family members, all these growth factors bind heparin and heparan sulphate. FGF-2 binding to heparan sulphate has been shown to reflect a complex biochemical regulatory mechanism for this growth factor [11].

2.9.2.1 *Properties*

FGF-2 was first identified as a 15 $kg.mol^{-1}$ protein that later found to be the 18 $kg.mol^{-1}$ primary form proteolytic product. Larger forms of FGF-2 (22, 22.5 and 24 $kg.mol^{-1}$) have also been identified, resulting from alternative CUG translation initiation sites. The homogeneous sequence for FGF-2 in many species is very high (> 90%). FGF-2 contains four cysteine residues without intramolecular disulfide bonds, many basic residues (p I = 9.6) and two sites (Ser 64 and Thr 112) that can be phosphorylated by protein kinases A and C. FGF-2 consists of 12 antiparallel β-layers arranged in a trigonal pyrimidal structure. While the binding of heparin and heparan sulfate has little effect on the structure of FGF-2, it can facilitate the self-association of FGF-2 molecules into higher order dimers and oligomers [11].

2.9.2.2 *Secretion from cells*

One of the most prominent features of FGF-2 is the absence of a consensus signal sequence for secretion. While the 18 $kg.mol^{-1}$ form of FGF-2 is found outside the cell of the higher molecular weight form, it is predominantly localized in the nucleus. The localization of high molecular weight FGF-2 is due to the extension of the amino terminus, which contains several Gly + Arg repeats with methyl residues. The mechanism of 18 $kg.mol^{-1}$ FGF-2 secretion remains unclear. It does not cross the endoplasmic reticulum or the Golgi via a regular pathway, but secretion is likely to occur during cell damage and death [11].

2.10 Release of proteins and drugs from PLGA-PEG based copolymers

In this thesis, the release of FGF2-stab from the thermosensitive PLGA-PEG-PLGA hydrogel was studied. PLGA-PEG-PEG-based hydrogels are ideal for the release of both hydrophobic and hydrophilic drugs since it is an amphiphilic compound that forms micelles in the aqueous

environment and the drugs have the ability to bind to either the hydrophobic nucleus or the hydrophilic surface of micelles.

Examples of release of proteins from copolymers based on PLGA-PEG segments that have already been studied are described below.

2.10.1 Protein release from PLGA-PEG-PLGA depending on changes in segment ratios

The rate of protein release can be adjusted by the ratio of PLGA/PEG segments. Since most proteins exhibit amphiphilic character (hydrophobic and hydrophilic) by adjusting the ratios of PLGA (hydrophobic) and PEG (hydrophilic) segments, release patterns are affected.

For example, the low molecular weight PEG segment of the PLGA-PEG-PLGA copolymer shows a low initial release of lysozyme (less than 10% in 48 hours) and a sustained release over 36 days. The di-block copolymer with a lower PEG content (10%) showed a lower initial release, but the remaining release was discontinuous and showed a significant second phase of rapid release due to polymer erosion. On the other hand, a higher PEG segment content (15%) caused a very rapid release of lysozyme [54], [55].

2.10.2 The effect of hydrophobicity on release from PLGA-PEG-PLGA hydrogel

The hydrophobic or hydrophilic nature of the drug release profile is relevant. The triblock PLGA-PEG-PLGA copolymer is often used for the controlled delivery of hydrophobic drugs as they form micelles in the aqueous environment and are able to bind drugs to their nuclei. When comparing the release of hydrophilic (paracetamol) and hydrophobic (sulpathiazole), it has been found that due to the binding of the hydrophobic drug to the core of the micelles it is released over a longer period (about half the time) than the hydrophilic paracetamol [31], [32], [49].

By comparing the release mechanisms of hydrophilic 5-fluorouracil and hydrophobic indomethacin, it was found that the hydrophilic drug was released by diffusion while the hydrophobic drug exhibited a two-step profile involving the initial phase-controlled diffusion followed by the erosion dominating hydrogel stage (see Fig. 15)[56].

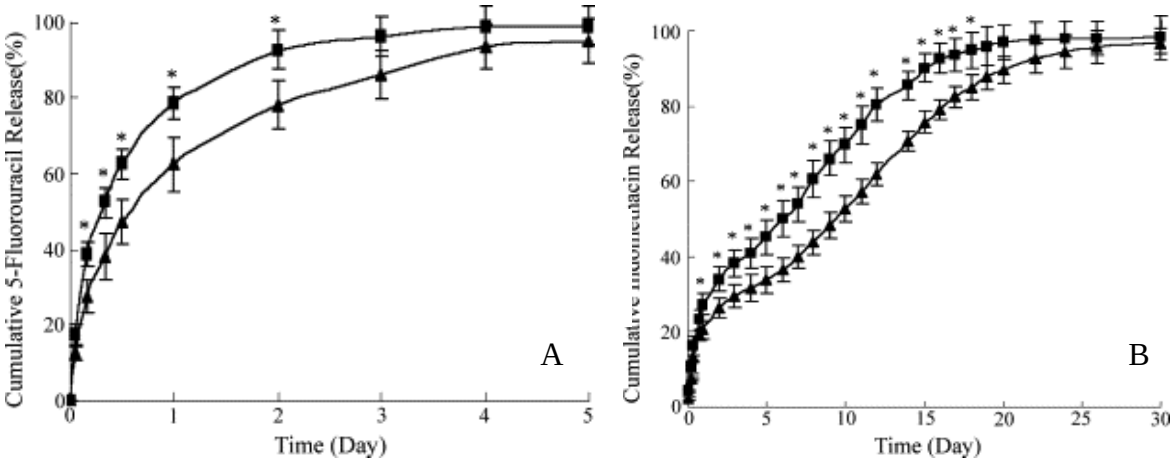

Fig. 15: Difference in drug release depending on hydrophobic character A) hydrophilic 5-fluorouracil exhibits single-stage release B) hydrophobic indomethacin exhibits two-stage release [56].

2.10.3 Modification of PLGA-PEG-PLGA copolymer

An example is the release of peptide drugs from the thermosensitive triblock copolymer of poly (ε-caprolactone-*co*-p-dioxanone)-*b*-poly(ethylene glycol)-*b*-poly(ε-caprolactone-*co*-*p*-dioxanone) (PECP) modified with jantoric anhydride thereby obtaining carboxyl groups at the chain ends. Modified HOOC-PECP-COOH copolymer displayed and retarded release profile for leuprorelin acetate over one month while effectively avoiding the initial burst, see Fig. 16. Controlled release is believed to be related to the formation of conjugated copolymer-peptide pair by ionic interaction and increased solubility of drug molecules in the hydrophobic hydrogel domains. Therefore, the carboxyl group hydrogel HOOC-PECP-COOH is a promising and well-exposed sustained-release carrier for peptide drugs, preferably being able to develop an injectable formulation by simple mixing [53].

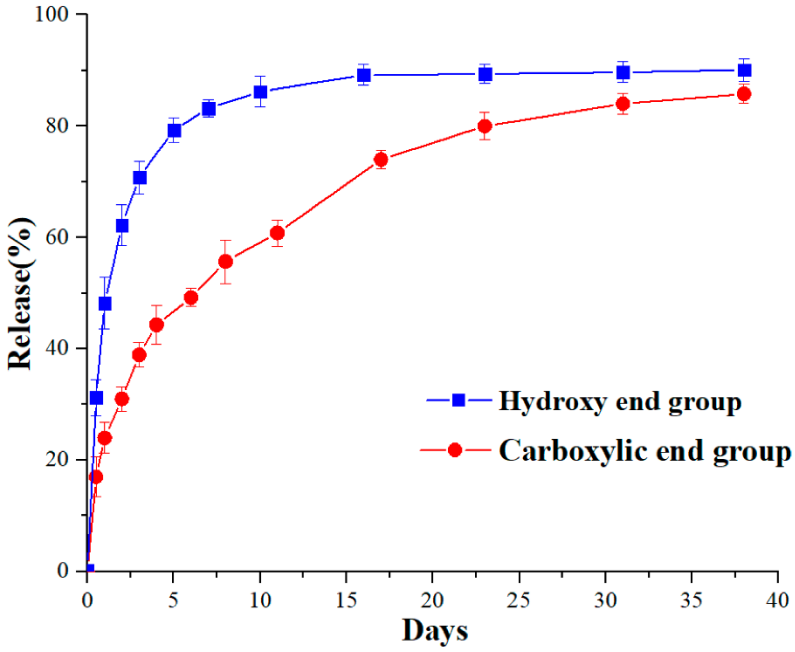

Fig. 16: A graph showing the comparison of release of leuprorelin acetate depending on the end of the string. When the blue curve shows the release from the OH-terminated copolymer and the red curve shows the release from the COOH-terminated copolymer

The PLGA-PEG-PLGA triblock copolymer terminated with itaconic acid offers reactive double bonds to. It is a modification with itaconic anhydride, which is an unsaturated cyclic anhydride. It is obtained by fermenting polysaccharides using Aspergillus terreus bacteria [21], [24].

PLGA-PEG-PLGA copolymer is modified by itaconic anhydride in “one-pot” reaction. Itaconic anhydride is bonded to the copolymer by ring-opening reaction, where itaconic acid is formed at the ends of the copolymer with reactive double bonds. These bonds are intended for both chemical crosslinking and carboxyl groups are suitable for reaction with biologically active substances. The modified ITA copolymer becomes sensitive to light, heat and pH [21], [24].

The presence of COOH groups may serve to prolong the release time with a reduction in the release of large amounts at the start of the measurement.

3 MAIN GOALS OF THE WORK

The main goal of the diploma thesis is method optimization for reproducible detection of released fibroblast growth factor from a hydrogel based on the thermosensitive PLGA-PEG-PLGA copolymer. And consequently, understanding the polymer-protein interactions to set optimal parameters providing controlled release of healing proteins.

Experimental part consists of:

1. Well-defined PLGA-PEG-PLGA copolymer synthesis via ring opening polymerization technique under inert atmosphere on a high vacuum all-glass line.
2. Chemical and physical PLGA-PEG-PLGA characterization in terms of gel permeation chromatography and rheology, respectively.
3. Measurement of FGF2-stab release from thermosensitive PLGA-PEG-PLGA hydrogel by vials-based Method A
4. Measurement of model proteins (lysozyme, albumin) and FGF2-stab release from thermosensitive PLGA-PEG-PLGA hydrogel by inserts-based Method B

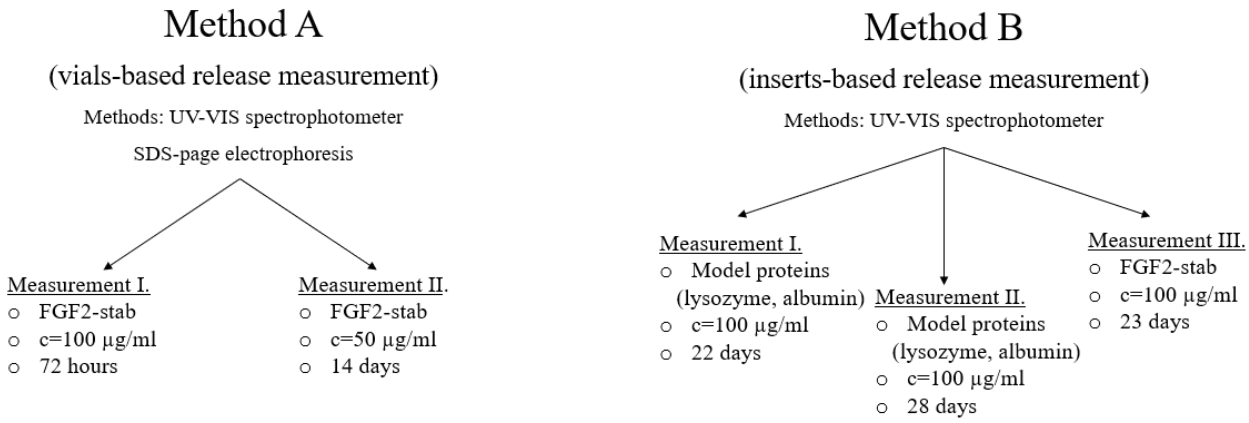

Fig. 17: Diagram of all measurements performed in the experimental part

4 EXPERIMENTAL PART

4.1 Chemicals

- Polyethylene glycol (PEG) with weight average molecular weight (M_w) of 1500 $g.mol^{-1,}$ was purchased from Sigma-Aldrich (Germany)
- D,L-Lactide (LA, ≥ 99.5%) was purchased from Polysciences (PA, USA)
- Glycolide (GA, ≥ 99.9%) was purchased from Polysciences, (PA, USA)
- Stable fibroblast growth factor (FGF-2 stab) was received from company Enantis, L.t.d. (Brno, Czech Republic)
- Albumin human (≥ 96%) was purchased from Sigma-Aldrich (MO, USA)
- Bovine serum albumin standard (c = 2 $mg.ml^{-1}$) was purchased from ThermoFisher Scientific (Netherlands)
- Lysozyme human (≥ 90%) was purchased from Sigma-Aldrich (MO, USA)
- Tin octanoate (SnII 2-ethylhexanoate, ≥ 92.5%) was purchased from Sigma-Aldrich (MO, USA)
- Liquid nitrogen (99.999%) was purchased from Linde Gas, a.s. (Czech Republic)
- Ultrapure water (Ultrapure water of Type I according to ISO 3696) was prepared on Millipore purification system (MilliQ Academic, Millipore, France)
- Bradford Reagent (for 0.1-1.4 $mg.ml^{-1}$ protein) was purchased from Sigma-Aldrich (MO, USA)
- Tetrahydrofuran (THF for HPLC, ≥ 99.9%) was purchased from Sigma-Aldrich (Germany)
- Di-sodium hydrogen phosphate dodecahydrate (≥ 98%) was purchased from Lach-Ner, L.t.d. (Czech Republic)
- Potassium dihydrogen phosphate (≥ 99%) was purchased from Lach-Ner, L.t.d. (Czech Republic)
- Potassium chloride (≥ 99%) was purchased from Sigma-Aldrich (MO, USA)
- Sodium chloride (≥ 99.5%) was purchased from Lach-Ner, L.t.d. (Czech Republic)
- Coomassie Brilliant Blue R ($C_{45}H_{44}N_3NaO_7S_2$) was purchased from Sigma-Aldrich (MO, USA)

4.2 Equipment

- UV-VIS Spectrophotometer V-730 (Jasco, Japan)
- Rheometer AR-G2 (TA instruments, USA)
- Analytical scales Adventurer Pro AV64 (OHAUS, Switzerland)
- Proton Nuclear Magnetic Resonance - 700 MHz NMR spectrometer Bruker AVANCE III at Masaryk University (Bruker Co., Germany)
- Cell Cultural Incubator CO2cell (BMT Medical, Czech Republic)
- Automatic pipettes (Hirschmann Laborgeräte, Germany)
- Lyophilizator /Freeze Dryer Epsilon 2-10D LSC plus (Martin Christ, Germany)
- Water proof pocket-size pH Meter S2K712 with ISFET sensors (ISFET Company, Japan)

- Gel permeation chromatography (HPLC GPC/SEC) 1260 Infinity (Agilent, CA, USA) with MALS (Multi-angel light scattering) photometry DAWN HELIOS-II WH2-02 (Wyatt, CA, USA) and refractometer T-rEX (Wyatt, CA, USA)
- WTW Spectroflex 6600 (Prolabmas, Indonesia)
- SPLInsert™ Hanging, 6 Inserts/6 well plate, PC, 0.4µm, Growth Area 4.52, 1.5~2.5ml, Opaque, Sterile6/24 (iBiotech, Czech Republic)
- PowerPac™ Basic Power Supply (Bio-Rad, Czech Republic) and Mini-PROTEAN® Tetra Vertical Electrophoresis Cell (Bio-Rad, Czech Republic)
- Thermo Block HLC (Ditabis, Germany)

4.3 Sample preparation

4.3.1 Synthesis and purification of PLGA-PEG-PLGA copolymer

The PLGA-PEG-PLGA triblock copolymer (ABA type) with a D, L-LA/GA molar ratio of 3.0 and a PLGA/PEG weight ratio of 2.5 was prepared by ring opening polymerization (ROP) under a nitrogen atmosphere. The reaction was carried out using a tin catalyst (Sn(II) 2-ethylhexanoate) at 130 °C for 3 hours [21].

The resulting product was purified from unreacted monomer by dissolving in ultra-pure water in a refrigerator at 3 °C and then rapidly heating to above 80 °C. The precipitated polymer was separated by decantation and purifying was repeated three times. The final product was freeze-dried [21].

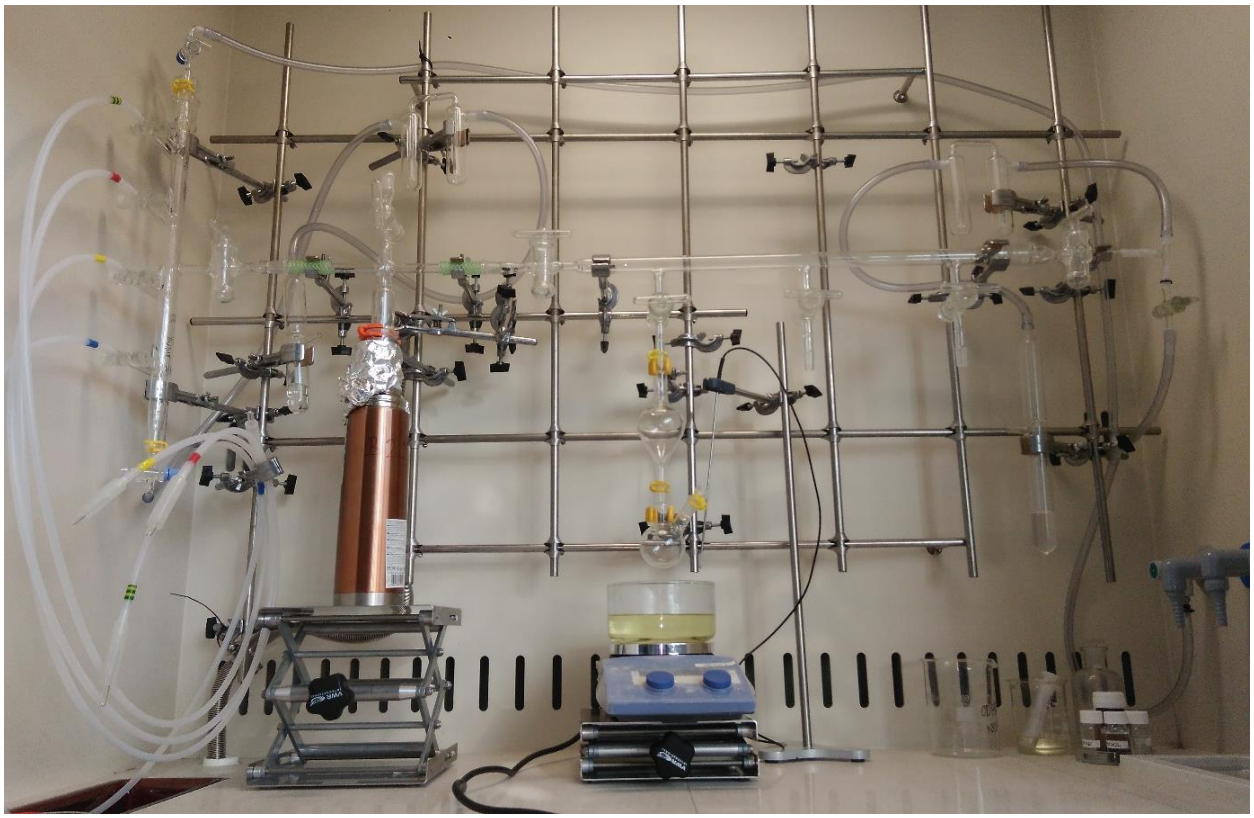

Fig. 18: Vacuum line for synthesis of thermosensitive copolymer (PLGA-PEG-PLGA).

4.3.2 Preparation of PLGA-PEG-PLGA copolymer solution

Two different concentrations of PLGA-PEG-PLGA copolymer aqueous solutions were prepared. 15 w/v % solution to measure rheological properties and 10 w/v % solution to measure the release of the protein, which was subsequently used as a gel matrix. For the rheological analysis, polymers were dissolved in ultra-pure water or in phosphate buffered saline (PBS). For the protein release measurement, copolymers were dissolved in PBS only. All solutions were prepared in the refrigerator at a temperature of 3 - 5 °C while stirring.

4.3.3 Sample preparation for monitoring the release from the thermosensitive hydrogel

Method A

In the measurement by method A, 10 w/v % ABA solution was mixed with 10% protein solution (with the concentration of 1 $mg.ml^{-1}$). The mixture was stirred for 30 min in a refrigerator at 4 °C, 30 min at room temperature and then allowed to gel for 45 min in an incubator at 37 ° C. 2 ml of phosphate buffer was dosed into the resulting gel to where the protein was released. Fig. 19 shows the sample preparation scheme. One sample was prepared for each measurement and the entire volume of PBS was collected after certain times. Fig. 20 shows a sample ready for the measurement. Due to the fast polymer degradation and hydrogel dissolution, the protein-solution withdrawing become more and more difficult. Moreover, degraded polymer negatively influenced the UV-VIS protein release measurement.

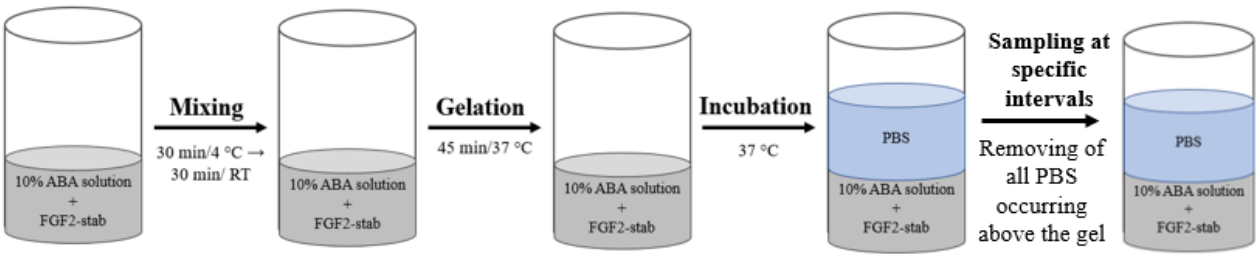

Fig. 19: Sample preparation scheme for measurement by method A.

Fig. 20: Prepared sample to measure FGF2-stab release by Method A – turbid gel on the vial bottom covered with clear PBS solution.

Method B

In the measurement by method B, cultivation plate inserts were used (see Fig. 22). In this case, proteins were released into the trays through the membrane while degraded polymer cannot go through to. The course of sample preparation was the same as in the measurement by method A, with only one difference that the gel was transferred to the insert after the solution was gelled. Protein release occurred across the membrane into the PBS-containing tray, which was always withdrawn over a given time period throughout the volume and the same amount of new PBS was dosed into the tray. A sample preparation scheme for measurement by method B is shown in the Fig. 21.

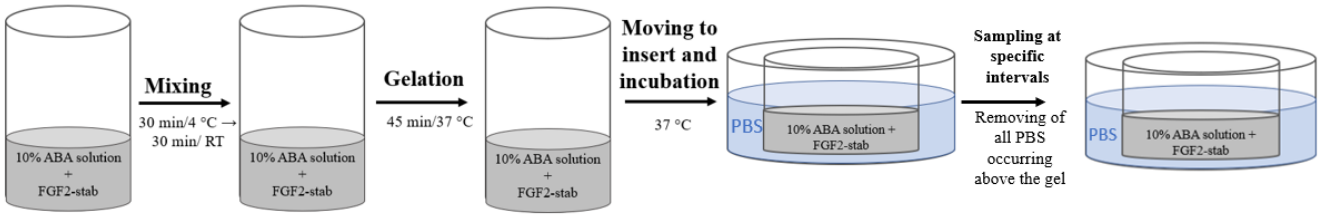

Fig. 21: Sample preparation scheme for measurement by Method B.

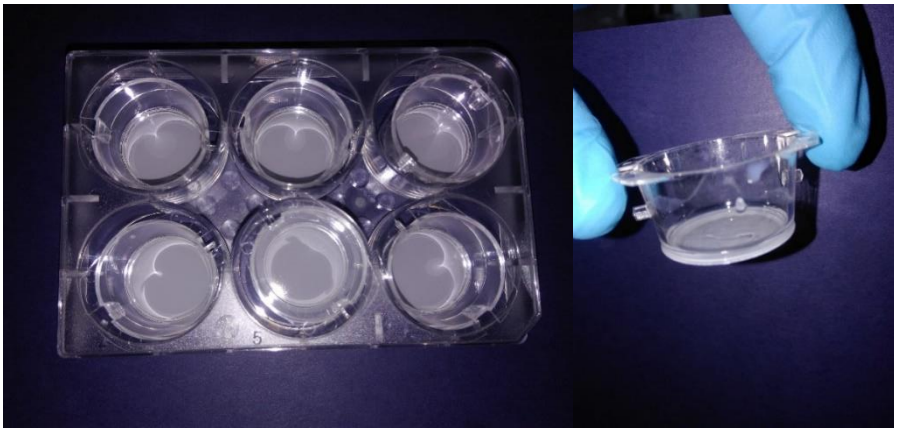

Fig. 22: Inserts used to release proteins as measured by Method B.

4.4 Methods

4.4.1 Gel Permeation Chromatography (GPC)

Gel permeation chromatography was used to determine the number average molecular weight (M_n) and polydispersity index (M_w/M_n). Two PLgel 5 µm Mixed-C columns were used for separation and tetrahydrofuran (THF) with a flow rate of 1 $mL.min^{-1}$ was used as the mobile phase. An analytical standard for GPC/SEC polystyrene (PS) with a molecular weight of M_w = 30.000 $g.mol^{-1}$ and PDI = M_w/M_n = 1.06 was used as standard to calibrate the system, however, obtained data were absolute due to the set-up of detectors. All measured data were evaluated using Astra software.

Fig. 23: 1260 Infinity gel permeation chromatography with MALS and refractometer detectors used for measurement.

4.4.2 Proton Nuclear Magnetic Resonance

Molecular weight and polymer characterization results were confirmed using proton nuclear magnetic resonance ^1H NMR spectroscopy on 700 MHz Bruker AVANCE III HD instrument using 128 scans in deuterated chloroform ($CDCl_3$) solvent at 25 °C. Chemical shifts were reported in ppm relative to tetramethylsilane (TMS). ^1H NMR spectra were evaluated using ACD/1D NMR Processor.

Fig. 24: Proton Nuclear Magnetic Resonance - 700 MHz NMR spectrometer Bruker AVANCE III used for measurement.

4.4.3 Dynamic Rheological Analyses

The rheological analysis was used to analyse the PLGA-PEG-PLGA triblock copolymer solution in order to determine the modulus of storage and the loss modulus, thereby determining the start of gelation of the copolymer solution together with the decay temperature of the gel. To measure the temperature dependence, a cone-plate geometry with a diameter of 40 mm and 2 ° angle was used. 600 µl of the copolymer solution was metered into the Peltier by syringe and the working position (geometric gap of 60 µm) was set. A water-filled solvent trap was used to prevent solvent evaporation during the experiment. The temperature ramp was set between 15 − 60 °C with a heating rate of 0.5 °C per minute. All measurements were made at a constant frequency of 1 rad. s^{-1} and 1% stain.

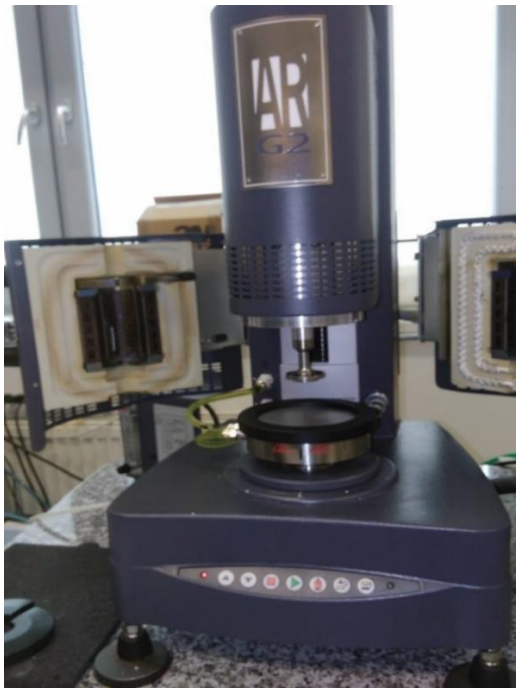

Fig. 25 : Rheometer AR-G2 (TA Instruments) used for the visco-elastic properties measurement.

4.4.4 SDS-PAGE electrophoresis

SDS-PAGE is a polyacrylamide gel electrophoresis in the presence of sodium dodecylsulphate way to identify and track proteins. SDS-PAGE is commonly used to determine molecular weights between 5 and 250 $kg.mol^{-1}$. The reducing agent (dithiothreitol, mercaproethanol) acts on the disulphide bonds within the protein structure, causing the quaternary structure of the proteins to break down into individual protein subunits that bind the high negative charge SDS molecules at a constant ratio of 1.4 g of SDS to 1 g of polypeptide. Proteins have a uniform negative charge due to bound amine detergent and their original charges become negligible. After insertion of the voltage, the SDS-polypeptide complexes formed are then separated in a polyacrylamide gel based solely on their size [7], [8].

This measurement was performed by company Enantis, L.t.d., the producer of FGF2-stab protein. The composition of the gel is shown in the Tab. 2.

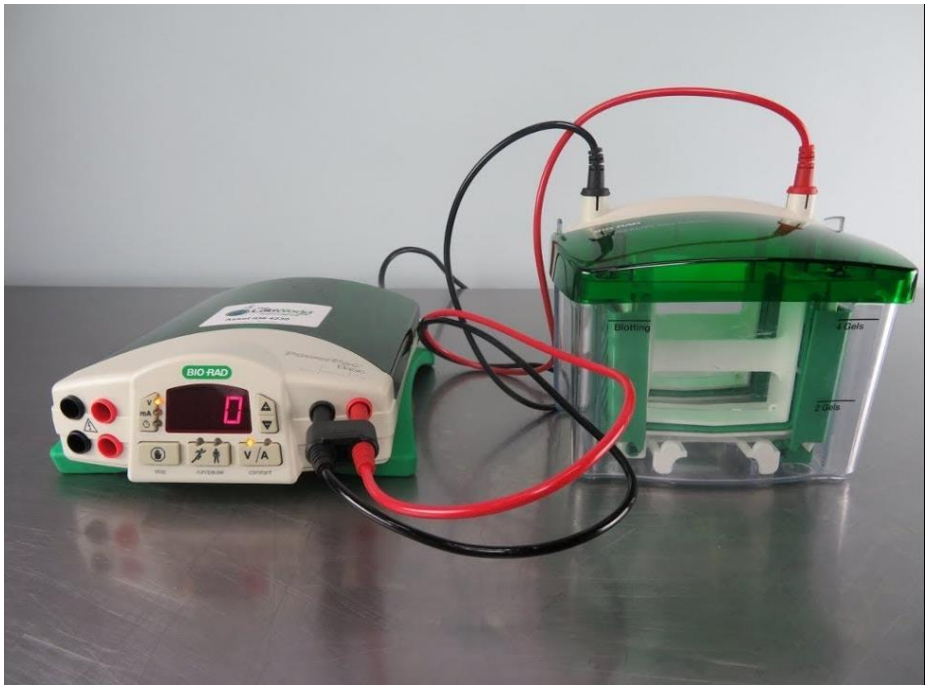

Fig. 26: Electrophoresis cell PowerPac™ Basic Power Supply and Mini-PROTEAN® Tetra Vertical Electrophoresis Cell (Bio-Rad) used for the protein release measurement.

Tab. 2: Composition of SDS gel

Resolving gel 15% to prepare 4 gels		**Stacking gel 5% to prepare 4 gels**	
Resolving buffer	4.6 ml	Stacking buffer	2 ml
Acrylamide 30%	9 ml	Acrylamide 30%	1.08 ml
MiliQ water	4 ml	Distilled water	4 ml
APS 10%	180 µl	APS 10%	120 µl
SDS 10%	180 µl	SDS 10%	80 µl
TEMED	14 µl	TEMED	10 µl
Resolving buffer (1.5 M Tris-HCl, pH 8.8)		Stacking buffer (0.5 M Tris-HCl, pH 6.8)	

4.4.5 UV-VIS spectroscopy with Bradford reagent

The UV-VIS spectrophotometer was used to measure the amount of released proteins from the thermosensitive hydrogel. The measurement was carried out at a constant wavelength of 595 nm. A Bradford reagent that interacts with proteins was used to shift absorption maxima from 280 nm to 595 nm. Quartz cuvettes were used in which the ratio of Bradford reagent to sample was dosed according to the expected amount of released protein with the selected calibration curve. Reagent/sample ratios and pipetted volume are shown in the Tab. 3.

Tab. 3: Reagent / sample pipetted volume and ratio

	Bradford agent [ml]	Sample [ml]	Bradford agent	Ratio	Sample
Low concentration (1-10 µg/ml)	1.3	1.3	1	:	1
Middle concentration (10-100 µg/ml)	2	0.5	4	:	1
High concentration (100-1 000 µg/ml)	2.5	0.075	33.3	:	1

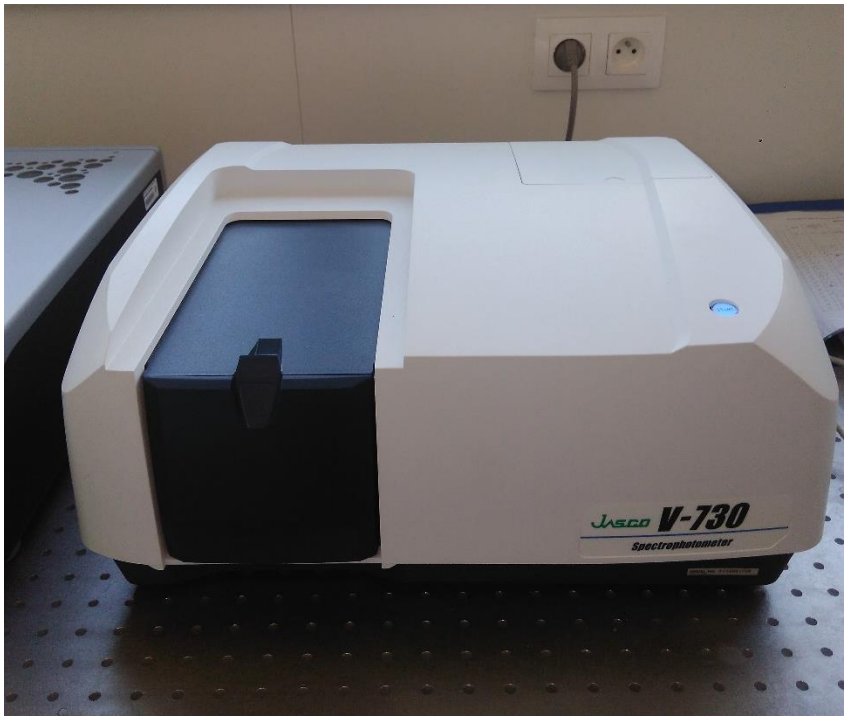

Fig. 27: UV-VIS spectrophotometer V-730 (Jasco) used for the release measurement.

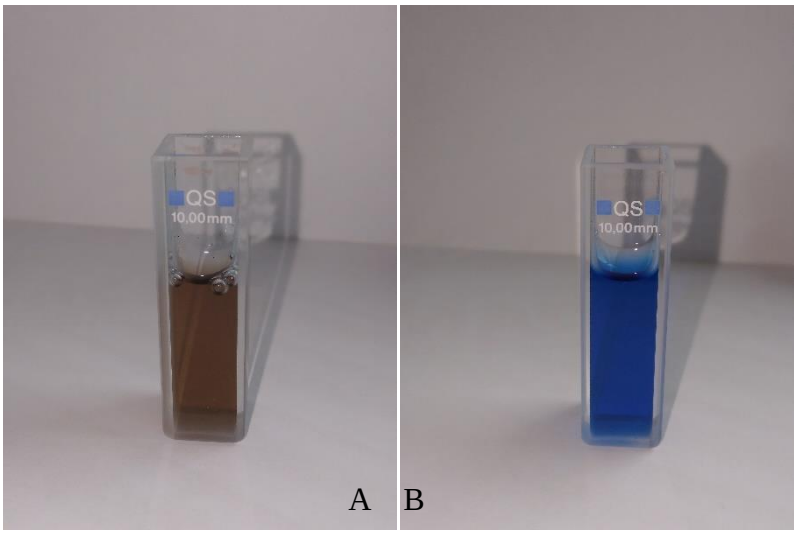

Fig. 28: A) Brown staining of unreacted Bradford reagent B) Blue stained cuvette with Bradford reagent in which agent-protein interaction occurred.

4.4.6 Enzyme-linked immunosorbent assay (ELISA)

Enzyme Immunosorbent Analysis (ELISA) is a technique used to detect the presence of antibody or antigen in samples. There are several different types of ELISAs, including indirect, sandwich, competitive and reverse ELISAs. All this can be used to detect proteins, viruses and drugs. This assay can be used to analyse a specific analyte or screen groups of compounds that cross-react with an antigen that is coated on a solid surface. The process first involves adding the sample of interest to the antigen coated on the microtiter plate. An antibody that is bound to the enzyme is then added to the antigen. Antibody reaction to antigen produces a fluorescent antigen / antibody complex that is detectable by ultraviolet light. The optical density of each well in the microtiter plate is compared to the control samples. Even though background reduction, signal enhancement, or cross-reactivity are potential limitations to ELISA analyses, these assays demonstrate a high degree of specificity and sensitivity [51], [52].

ELISA measurement was performed by Enantis, L.t.d.

5 RESULTS AND DISCUSSION

5.1 Thermosensitive copolymer (PLGA-PEG-PLGA) characterization

Gel permeation chromatography (GPC) and rheological analysis were used to characterize all of the PLGA-PEG-PLGA copolymer batches used as protein release matrices. The ABA copolymer was synthesized according to Ing. Michlovská, Ph.D. dissertation thesis [48]. The prepared copolymer had a honey-like structure, beige semi-transparent colour as shown Fig. 29.

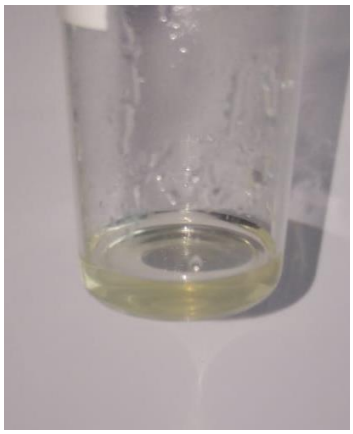

Fig. 29: Synthesized PLGA-PEG-PLGA copolymer after purification

5.1.1 Characterization of properties by gel permeation chromatography (GPC)

The peculiarity of polymers is that molar mass distribution occurs and thus we cannot obtain one molecular weight number. Gel permeation chromatography (GPC) or size exclusion chromatography (SEC) was used to determine number average molecular weight (M_n) and polydispersity (PDI). For measurement, 15 mg/ml PLGA-PEG-PLGA copolymer dissolved in tetrahydrofuran (THF) was dosed. In total, 5 batches of the produced ABA copolymer were used as a protein release matrices. Astra software was used to evaluate all data. PS of M_w = 30,000 g/mol and PDI = 1,06 were used as analytical standard. Each sample was measured twice for the control, see the graph where sample no 4 is displayed.

Tab. 4 shows a comparison of all results. The number average M_n was equal to 5 800 g.mol^{-1} having the polydispersity of 1,09. An example of a measured graph of the molecular weight distribution of the ABA copolymer (Sample No. 4) shows Fig. 30. Curve 1 describes the molecular weight distribution and curve 2 is Mark -Houwink plot which tells us that it is a linear polymer.

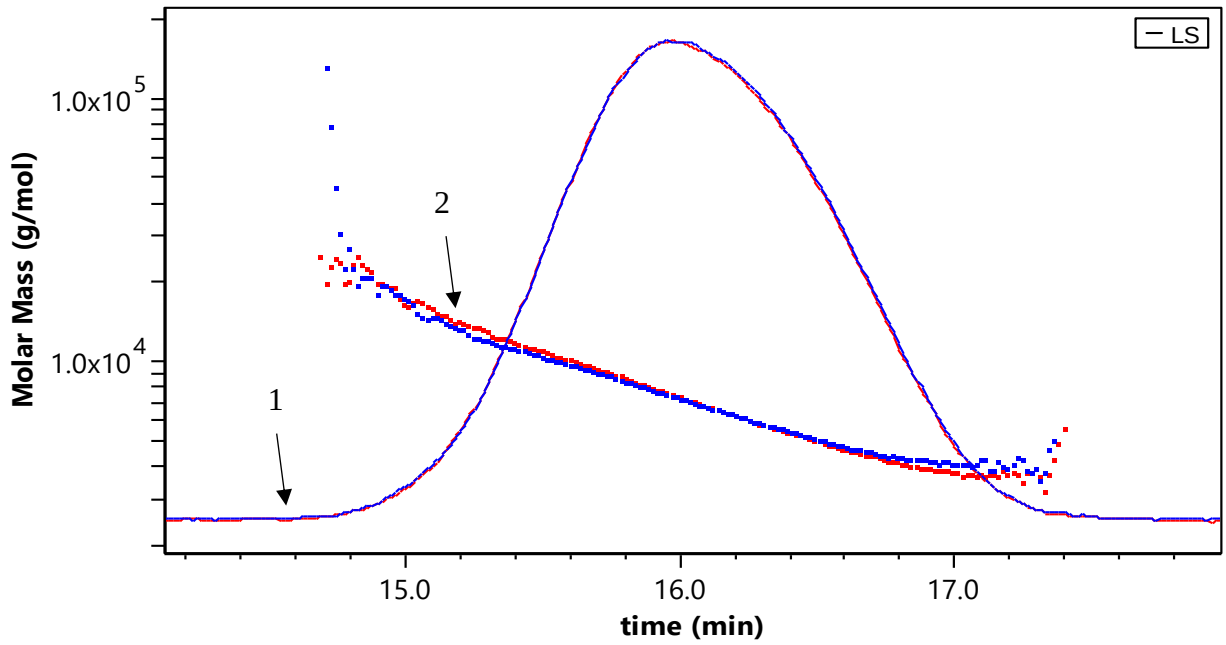

Fig. 30: Graph of molecular weight distribution of ABA copolymer measured by 1260 Infinity gel permeation chromatography with MALS and refractometer detector. Each sample was measured twice for the control, see the graph where sample no 4 is displayed.

Tab. 4: Results of average number molecular weight (M_n) and polydispersity (PDI) measurements of all batches of ABA copolymer used for sample preparation for release

Batch of ABA copolymer	1	2	3	4	5	Diameter
Number average molecular weight (M_n) [g.mol^{-1}]	5 820	5 713	5 597	5 987	5 779	5 779
Polydispersity (PDI)	1,056	1,092	1,096	1,095	1,086	1,085

5.1.2 Characterization of properties by ^{1}H NMR spectroscopy

PLGA-PEG-PLGA copolymer was characterized by ^{1}H NMR spectroscopy. Characteristic spectrum of PLGA-PEG-PLGA copolymer is shown in Fig. 31. Six peaks are observed in the spectrum, with the largest shift peak being chloroform, which was used as solvent. The peak with the lowest shift δ = 0.9 – 1.2 ppm (e) is characteristic of the lactic acid proton (O-(C**H**$_3$)CHO). The peak characteristic of (O-(CH$_3$)C**H**O) (d) is about δ = 5.1 – 5.3 ppm. The peak with shift in the area δ = 3.5 – 3.7 ppm is characteristic of the polyethylene glycol proton (OC**H**$_2$C**H**$_2$O) (d). By shifting in the area δ = 4.6 - 4.9 ppm there is a peak corresponding to the proton glycolic acid (OC**H**$_2$O) (b). The peak with the lowest intensity δ = 3.7 - 3.9 ppm corresponds to the proton between glycolic acid and lactic acid [50]. The PLGA/PEG weight ratio and LA/GA molar ratio were calculated. The copolymer was synthetized of PLGA/PEG weight ratio 2.5 and LA/GA molar ratio 2.91.

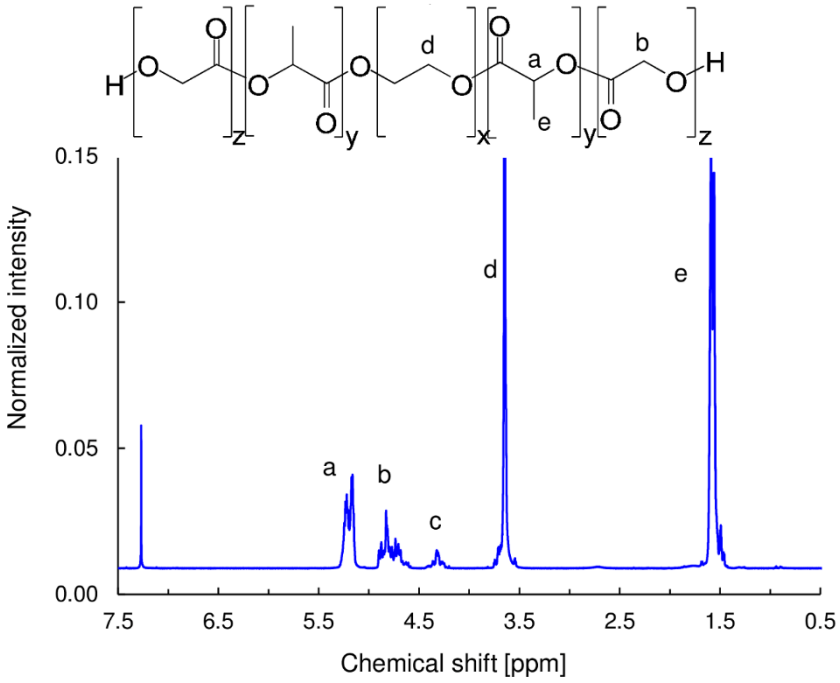

Fig. 31: NMR spectrum of PLGA-PEG-PLGA triblock copolymer.

5.1.3 Rheological properties characterization

The rheological analysis was used to confirm the temperature-dependent behaviour of the PLGA-PEG-PLGA copolymer. Because the copolymer consists of a hydrophilic PEG segment and a hydrophobic PLGA segment, the resulting structure has an amphiphilic character and thus forms micelles and gel in the aqueous environment. The composition of the ABA copolymer was adjusted to form a gel at physiological temperature. In this type of hydrogel, two transitions occur, namely the sol-gel transition (gelation temperature) and the breakdown of the gel structure. The gelation temperature was established at 31.2 °C by contacting the G′ and G′′ curves, see point 1 in Fig. 32. It is the temperature when the formation of a gel structure begins. The temperature at which the gel reached its highest strength was determined as the maximum value of the G′ curve and reached 37.2 °C. At point 2 in the Fig. 32, the crosses of the G′ and G′′ curves are seen when the elastic modulus falls below the loss mode and the gel breaks down. This decay occurs at 40 °C. A 15% solution of PLGA-PEG-PLGA copolymer dissolved in PBS was prepared for analysis. Phosphate buffer was used for reasons of later use of the buffer during protein release. The measurement was carried out in the temperature range of 15-55 ° C.

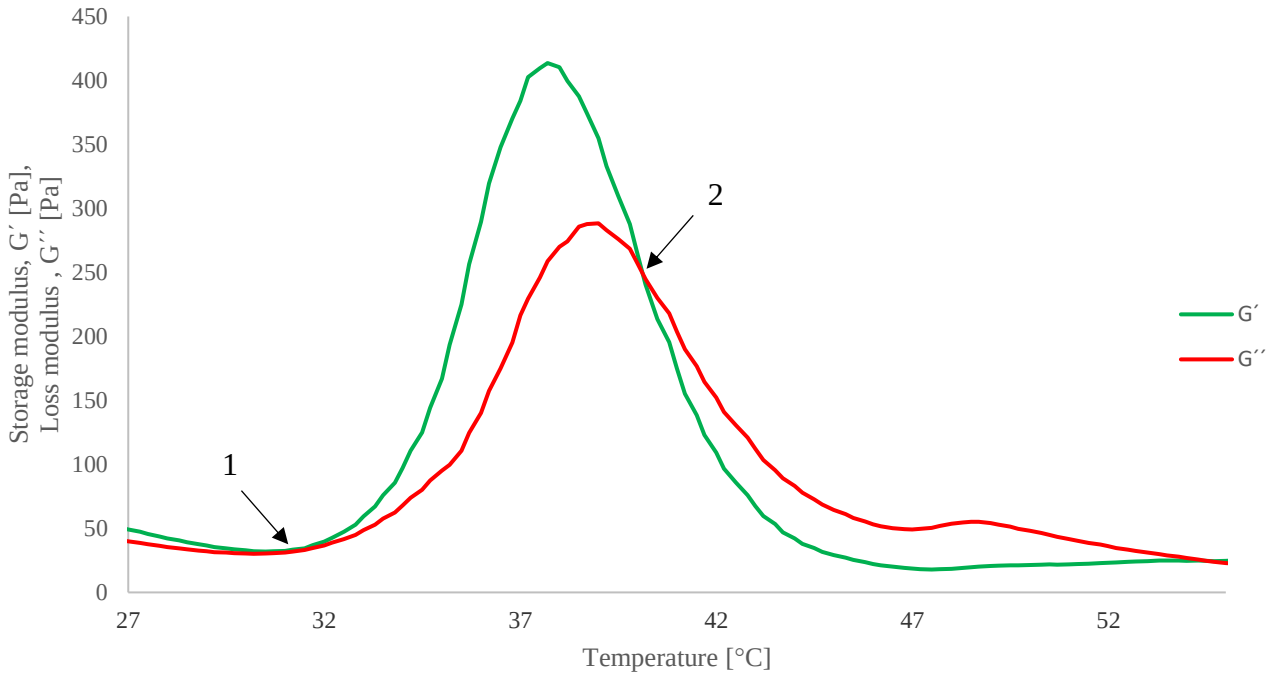

Fig. 32: Graph of temperature dependence of 15% PLGA-PEG-PLGA copolymer solution measured by AR-G2 Rheometer.

5.2 Release of proteins

For the protein release, we have used two type of measurement – Method A and Method B. In the Method A of measuring the release of stable Fibroblast growth factor 2 from the thermosensitive PLGA-PEG-PLGA copolymer, a 10% ABA gel solution dissolved in PBS with 10% FGF2-stab was used. Release proceeded from the gel that was at the bottom of the vial to PBS, which was above the gel and formed a visible interface (see Fig. 33, A). Method B is based on the measurement of model proteins (lysozyme, albumin) and FGF2-stab release from thermosensitive PLGA-PEG-PLGA hydrogel. The difference is the use of inserts, where proteins are released into PBS through the membrane and the influence of measurement by degrading gel is eliminated.

5.2.1 Method A of measurement of stable Fibroblast growth factor 2 (FGF2-stab) release (Measurement I.)

For the Measurement I., 5 samples with 10% FGF2-stab (c=100 µg/ml) content and 5 samples where FGF2-stab was replaced by buffer only and served as BLANK were prepared. All samples were left in an incubator at 37 ° C to mimic the temperature of the human body. Samples (one sample with FGF2-stab and one BLANK) were collected at 5, 10, 24, 48 and 72 hours. The entire volume of the buffer above the gel was pipetted. This buffer volume was used for UV-VIS spectrophotometer and SDS-page electrophoresis analyses.

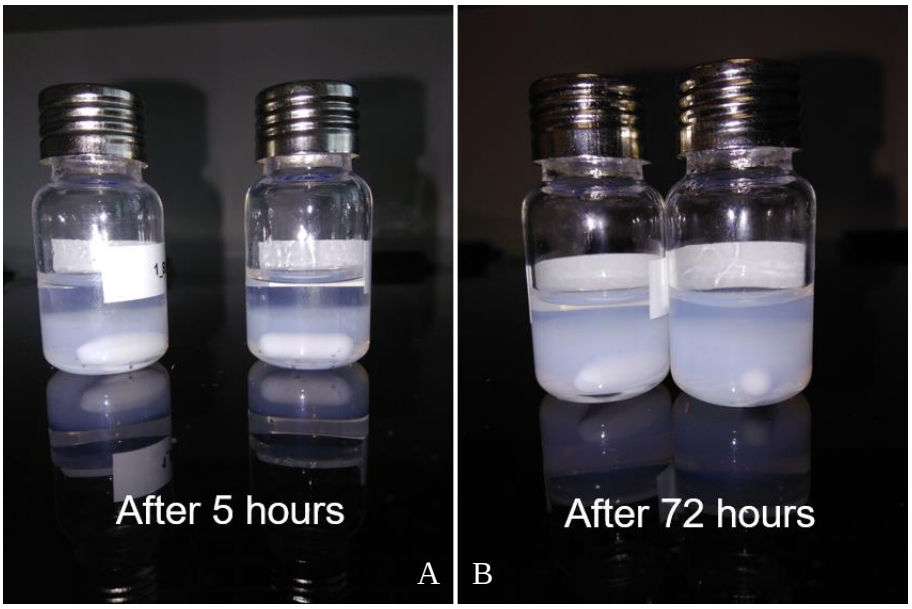

Fig. 33: Comparison of samples after removal from incubator at 37 ° C after 5 and 72 hours.

Measurement of the released amount of FGF2-stab using a UV-VIS spectrophotometer was performed in the presence of a Bradford reagent that shifts the maximum absorbance of the stable fibroblast factor 2 from 280 nm to 595 nm. Absorbance was measured for all samples and the concentration was calculated using calibration curves obtained from Enantis, L.t.d. The equation of the calibration curves is shown in the Tab. 5. Each sample (sample with both FGF2-stab and BLANK) was measured 3 times and since the absorbance was measured for BLANK, this value was always subtracted from the absorbance of the sample with FGF2-stab. The resulting concentrations were recalculated as the percentages of protein released, which are shown in the graph (see Fig. 34).

Tab. 5: Equation of the calibration curves obtained from Enantis, L.t.d. used in the method A

	Calibration curve equations
Low concentration (1-10 µg/ml)	y= 0.0312091x + 0.0148639
Middle concentration (10-100 µg/ml)	y= 0.0071849x + 0.0891212
High concentration (100-1 000 µg/ml)	y= 0.0007974x - 0.0043744

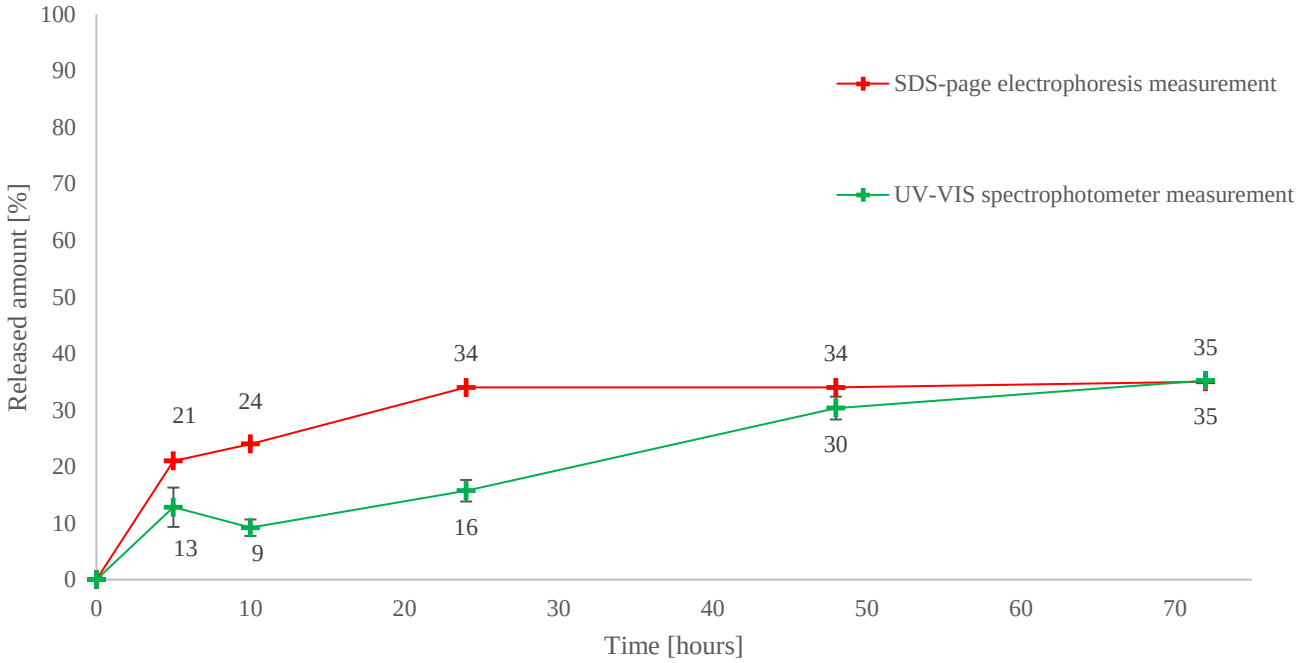

Fig. 34: Comparison of released amount of FGF2-stab from ABA gel measured by UV-VIS spectrophotometer and SDS-page electrophoresis.

SDS-page electrophoresis was used to verify the released amount of FGF2-stab measured by UV-VIS spectrophotometer. Samples were stained with dye (Coomassie Brilliant Blue R) and boiled for 5 minutes in a thermo-block at 95 ° C. The samples were dosed onto the gel and distributed using an electric field according to molar masses (see Fig. 36).

Tab. 6 shows the description of the samples in the Fig. 36. The band density was evaluated, and the concentration of stable fibroblast growth factor 2 was calculated using a calibration curve (see Fig. 35). Subsequently, the concentration was recalculated to percentages and plotted in the graph (see Fig. 34).

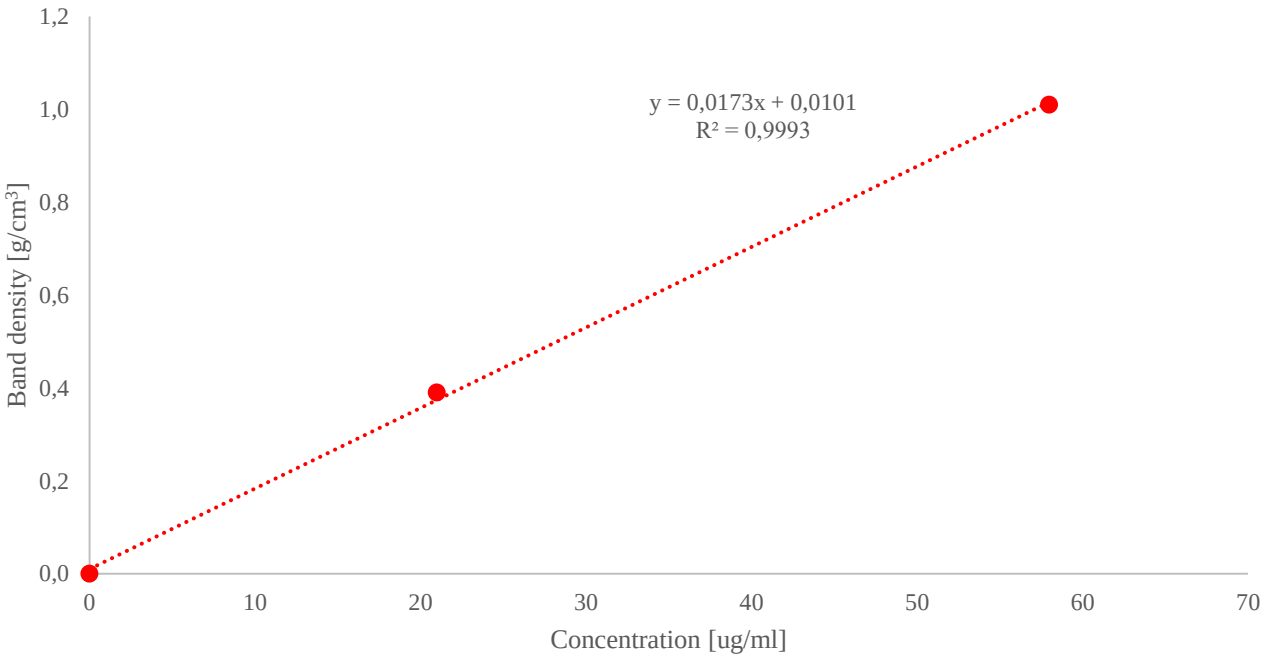

Fig. 35: Calibration curve to calculate the released amount of FGF2-stab from thermosensitive PLGA-PEG-PLGA hydrogel measured by SDS-page electrophoresis

By comparing the curves obtained using UV-VIS spectrophotometry and SDS-PAGE electrophoresis differences in the released amounts were observed (see Fig. 34). The total released amount was about 35% in 72 hours in both methods. Differences are visible mainly in samples taken at 5, 10 and 24 hours when UV-VIS spectrophotometer measurements are significantly lower (approximately 15%) than those measured by electrophoresis. This difference was probably due to subtraction of the absorbance by the degraded PLGA-PEG-PLGA copolymer in BLANKs samples from the absorbance of the FGF2-stab samples in UV-VIS spectrophotometry. In contrast, when measured by electrophoresis, the release of FGF2-stab was not affected by the degraded gel.

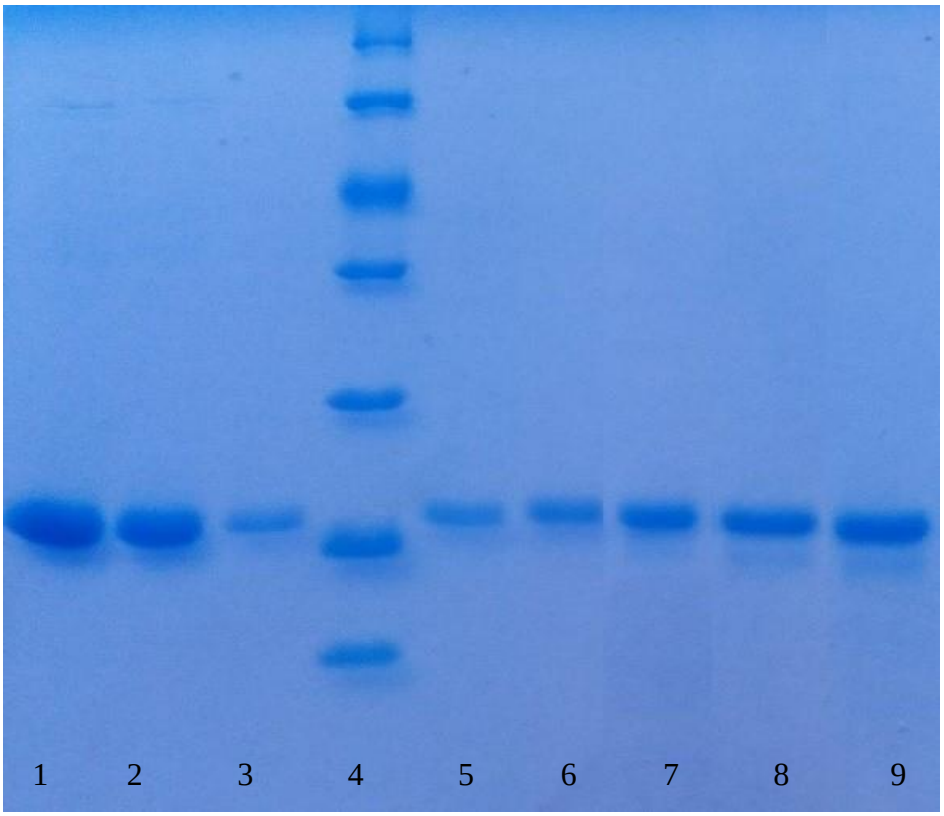

Fig. 36: Picture of gel of measured samples divided by molecular weight by SDS-page electrophoresis.

Tab. 6: Description of samples measured by SDS-page electrophoresis shown in the Fig. 36

Number	1	2	3	4	
Type of sample	FGF2 with concentration 130 µg/ml	FGF2 with concentration 58 µg/ml	FGF2 with concentration 21 µg/ml	SDS marker (14.4, 18.4, 25.0, 35.0, 45.0, 66.2 $kg.mol^{-1}$)	
Number	5	6	7	8	9
Type of sample	Sample measured after 5 hours	Sample measured after 10 hours	Sample measured after 24 hours	Sample measured after 48 hours	Sample measured after 72 hours

ELISA analysis was also performed by Enantis, L.t.d., but since this is a costly method and the results were affected by the degrading gel, this method was abandoned.

5.2.2 Method A of measurement of stable Fibroblast growth factor 2 (FGF2-stab) release (Measurement II.)

Due to the release of only 35% FGF2-stab in 72 hours at the Measurement I. in Method A, 18 samples were prepared for the Measurement II. (12 samples with FGF2-stab and 6 BLANKS). For comparison, 2 samples with FGF2-stab and 1 BLANK were measured every time. The collection period was extended to 14 days. Preparation, collection and measurement of the

samples were the same as in the first case. The only change was the concentration reduction FGF2-stab from c = 100 µg/ml to 50 µg/ml due to the high cost of FGF2-stab. Samples were taken from the incubator after 10 hours and then after 1, 3, 7, 10 and 14 days.

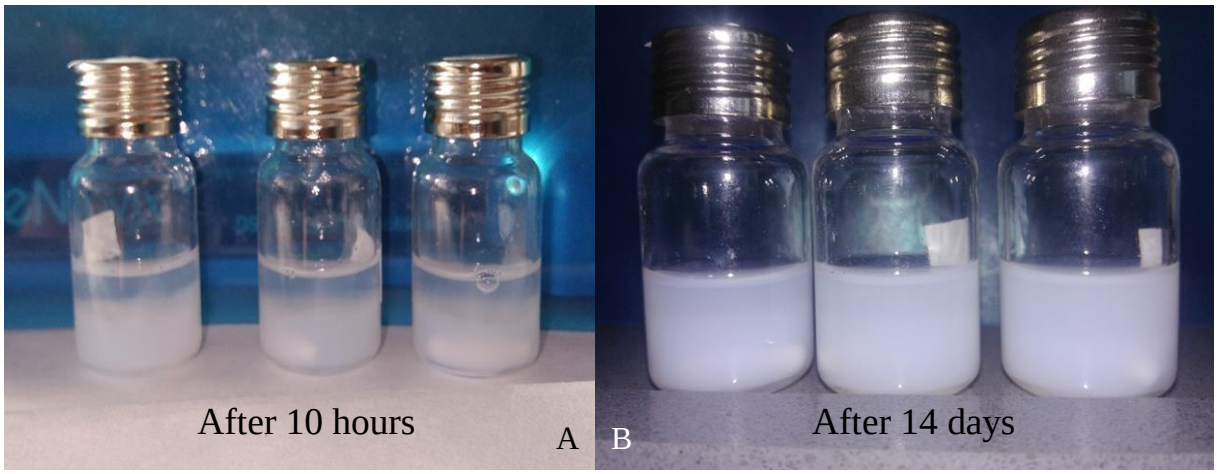

Fig. 37: Comparison of samples after removal from incubator at 37 ° C after 10 hours and 14 days.

The problem was the collection of phosphate buffer above the gel, whereby the ABA gel decomposed with increasing time and thus its strength was lost. Thus, the buffer and the disintegrated gel were mixed (see Fig. 37, B), and the UV-VIS spectrophotometer measurement was influenced.

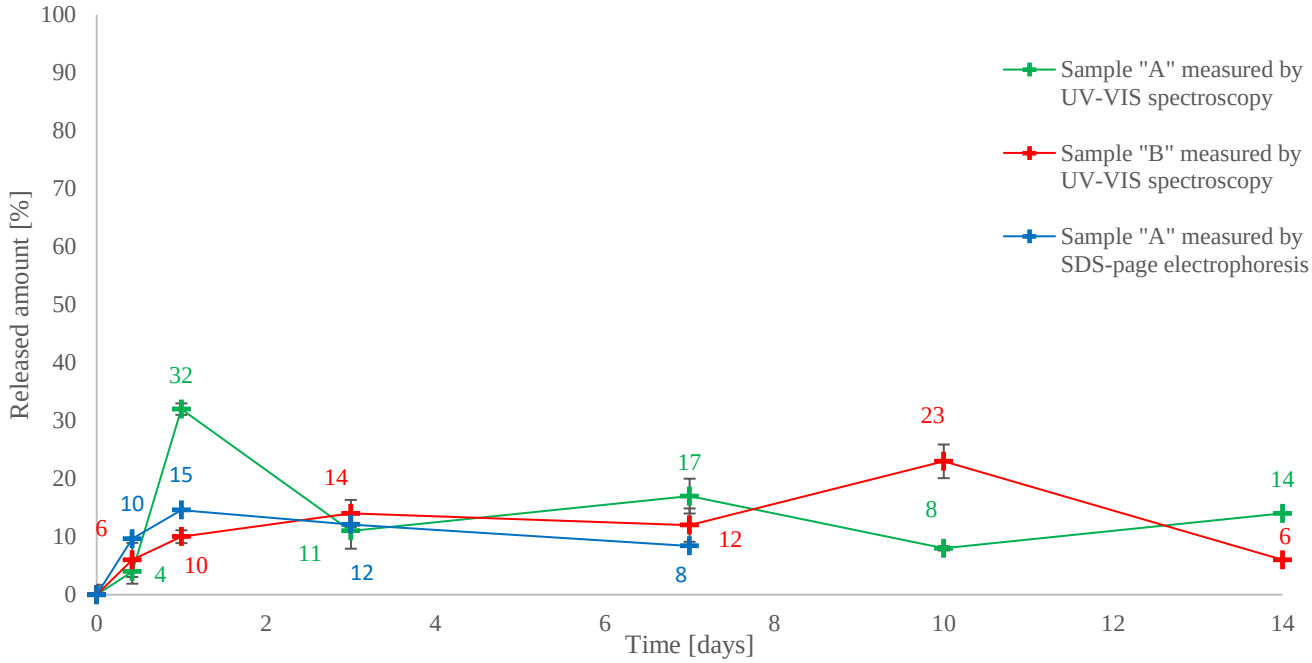

Fig. 38: Comparison of the released amount of two samples ("A" and "B") of FGF2-stab measured by UV-VIS spectrophotometer and one sample ("A") measured by SDS-page electrophoresis.

Significant differences were seen when comparing samples measured by UV-VIS spectrophotometry (see Fig. 38). For example, samples taken after 1 day were 22% of the difference in the amount released. Samples taken after 10 hours when the difference was only 2% were most comparable. These differences were due to the interaction of the disintegrated ABA gel with the Bradford reagent, and thus the measured absorbance was influenced. Because of this problem, no trend in the release has been observed.

Results obtained by evaluating SDS-page electrophoresis measurements were decreasing after 1 day. Due to the release of very low amounts of the samples were taken after 10 and 14 days under the detection limit (see Fig. 39 sample no. 8,9).

When comparing the I. and II. measurements, measurement II reduced the amount released due to the small amount (c = 50 µg/ml) of FGF2-stab mixed into the thermosensitive ABA hydrogel. While in the measurement I 35% was released after 72 hours for the measurement II, only 14% for the "A" sample and 6% for the "B" sample were measured after 14 Days.

Due to the hydrogel degradation and difficulties in withdrawing liquids with released protein, new Method B has been applied with well-plates inserts.

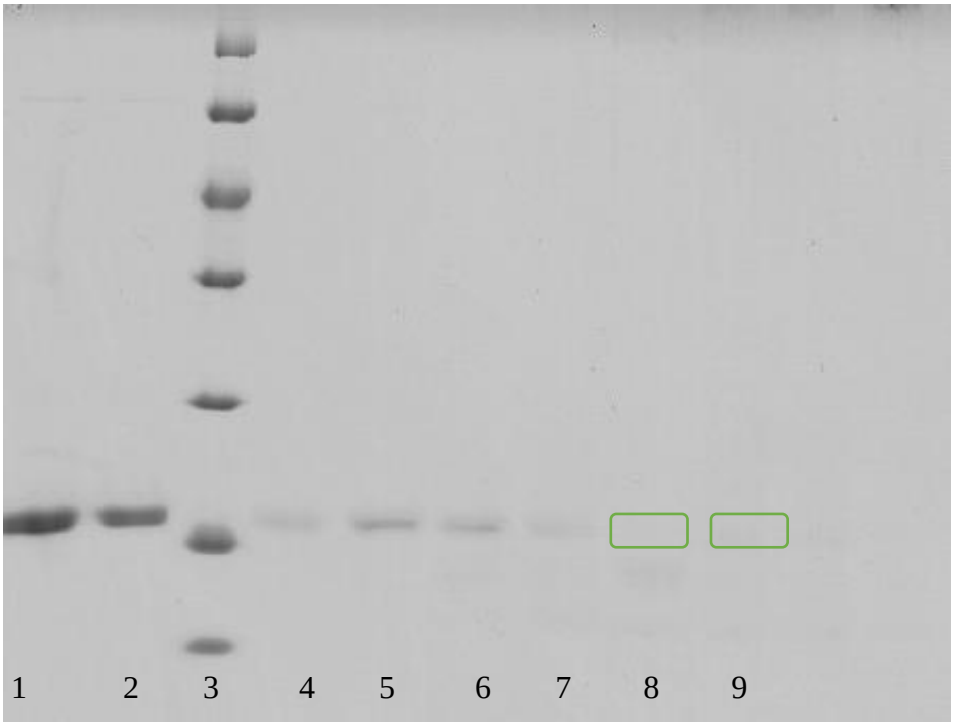

Fig. 39: Image of samples measured by SDS-page electrophoresis, when samples were below detection limit due to low concentration of mixed FGF2-stab into thermosensitive ABA gel.

Tab. 7: Description of samples measured by SDS-page electrophoresis shown in the Fig. 39

Number	1		2		3	
Type of sample	FGF2 with concentration 54 µg/ml		FGF2 with concentration 34 µg/ml		SDS marker (14.4, 18.4, 25.0, 35.0, 45.0, 66.2 $kg.mol^{-1}$)	
Number	4	5	6	7	8	9
Type of sample	Sample measured after 10 hours	Sample measured after 1 day	Sample measured after 3 days	Sample measured after 7 days	Sample measured after 10 days	Sample measured after 14 days

5.2.3 Method B insert-based release measurement

Due to significant influence on the measurements by disintegrated gel after longer time in the Method A of measurement was searched another variant how to FGF2-stab release from thermo-sensitive ABA gel measured. As a possible variant, the use of inserts (see Fig. 45) has been shown. There are two trays, one is smaller, with the membrane on the bottom, and second is larger. A gel with incorporated protein was dosed into the smaller tray and phosphate buffer was dosed into the larger bottom tray into which proteins were released through the membrane. Using the semipermeable membrane was significantly decreased interaction measurements by disintegrated gel which doesn´t pass through the membrane (see Fig. 46).

5.2.4 Calibration curves created to UV-VIS spectrophotometer for Method B measurement

Calibration curves were created to measure release of model proteins (lysozyme and albumin) for different concentrations. The measurement was carried out using a UV-VIS spectrophotometer at 595 nm, in the presence of a Bradford reagent that specifically binds to proteins and moves their absorption maxima from 280 nm, which is in the UV region, to 595 nm, which is in the ratio of the visible light.

Calibration curves were prepared for low concentrations, ranging from 1 to 10 µg/ml, middle concentrations, ranging from 10 to 100 µg/ml and high concentrations, ranging from 100 to 1 000 µg/ml. These calibration curves (see Fig. 40,Fig. 41, Fig. 42) were generated for the model proteins lysozyme and albumin. For Fibroblast growth factor 2, a calibration curves (see Fig. 43,Fig. 44) for low and middle concentrations were made using bovine albumin standard of the given concentration.

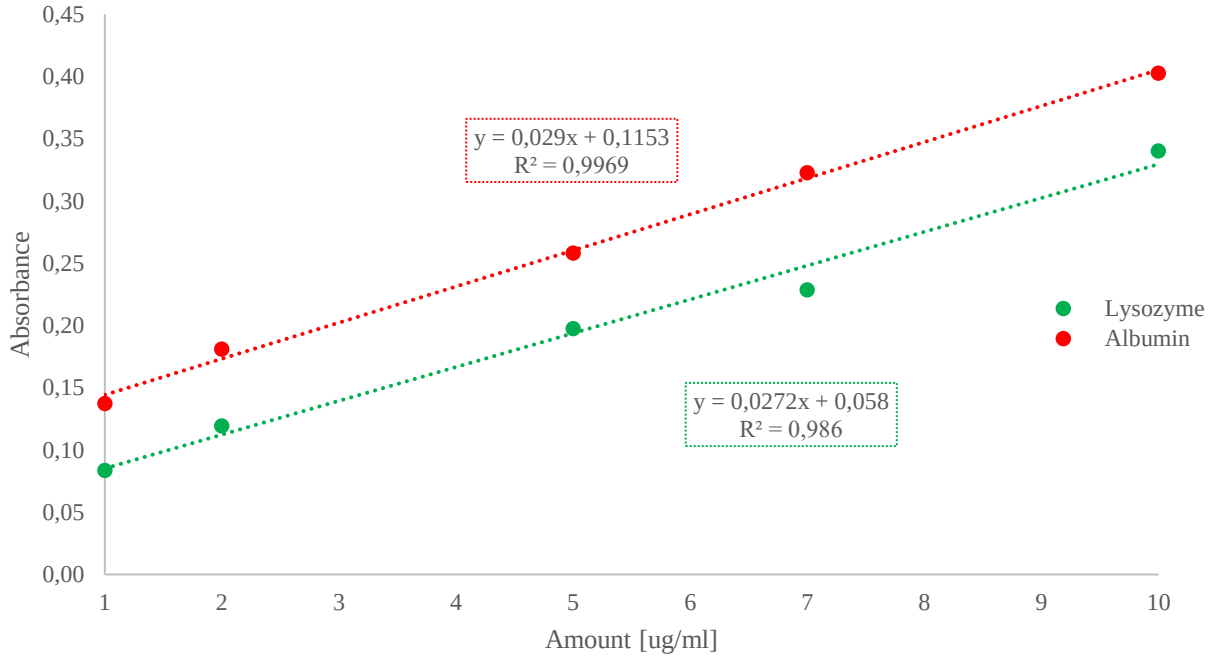

Fig. 40: Calibration curves created for lysozyme and albumin for low concentrations (1–10 µg/ml) measured by UV-VIS spectrophotometer at 595 nm in the presence of Bradford reagent.

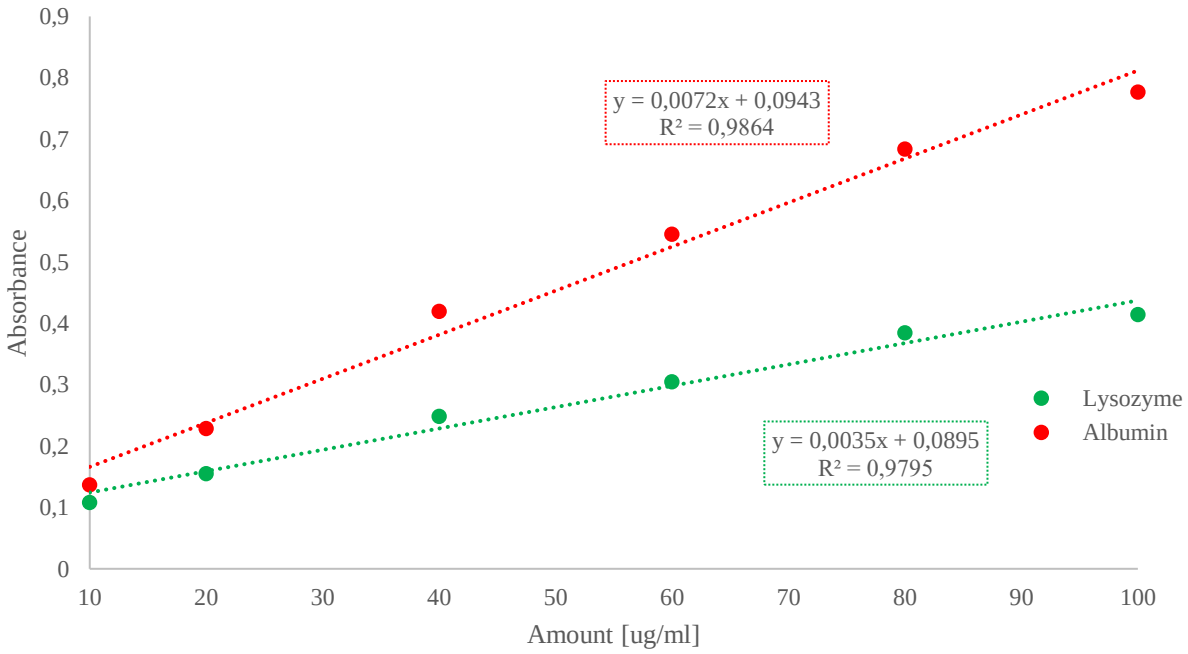

Fig. 41: Calibration curves created for lysozyme and albumin for middle concentrations (10–100 µg/ml) measured by UV-VIS spectrophotometer at 595 nm in the presence of Bradford reagent.

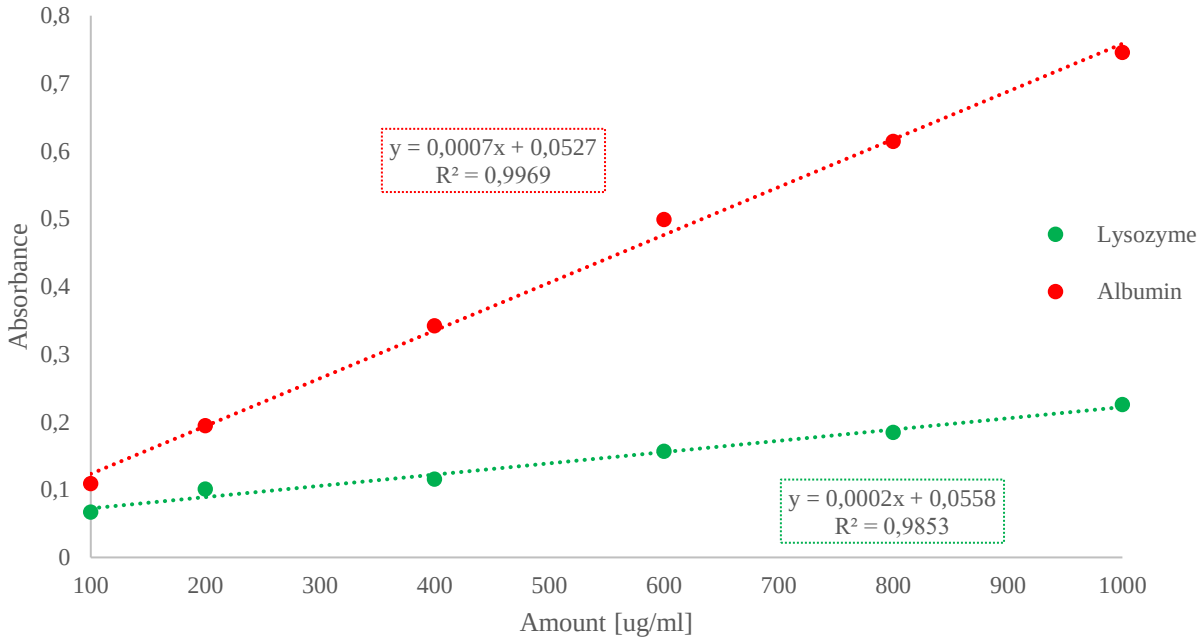

Fig. 42: Calibration curves created for lysozyme and albumin for high concentrations (100–1 000 µg/ml) measured by UV-VIS spectrophotometer at 595 nm in the presence of Bradford reagent.

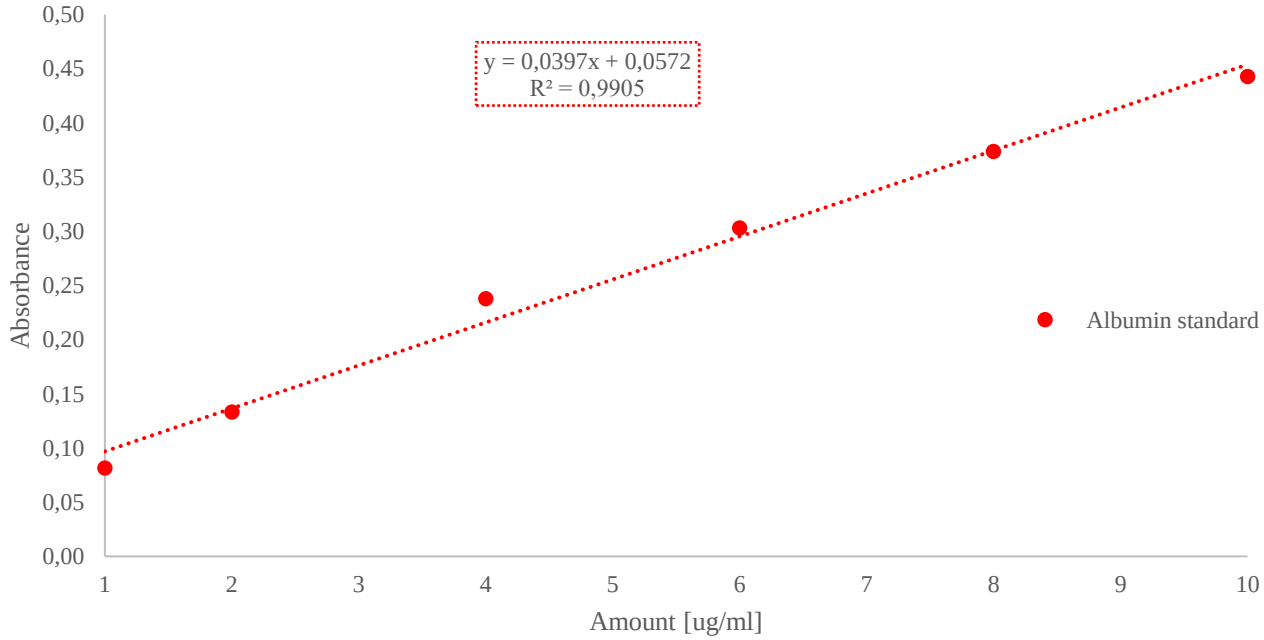

Fig. 43: Calibration curve measured for stable Fibroblast growth factor 2 using albumin standard at a given concentration for low concentrations (1–10 µg/ml) measured by UV-VIS spectrophotometer at 595 nm in the presence of Bradford reagent.

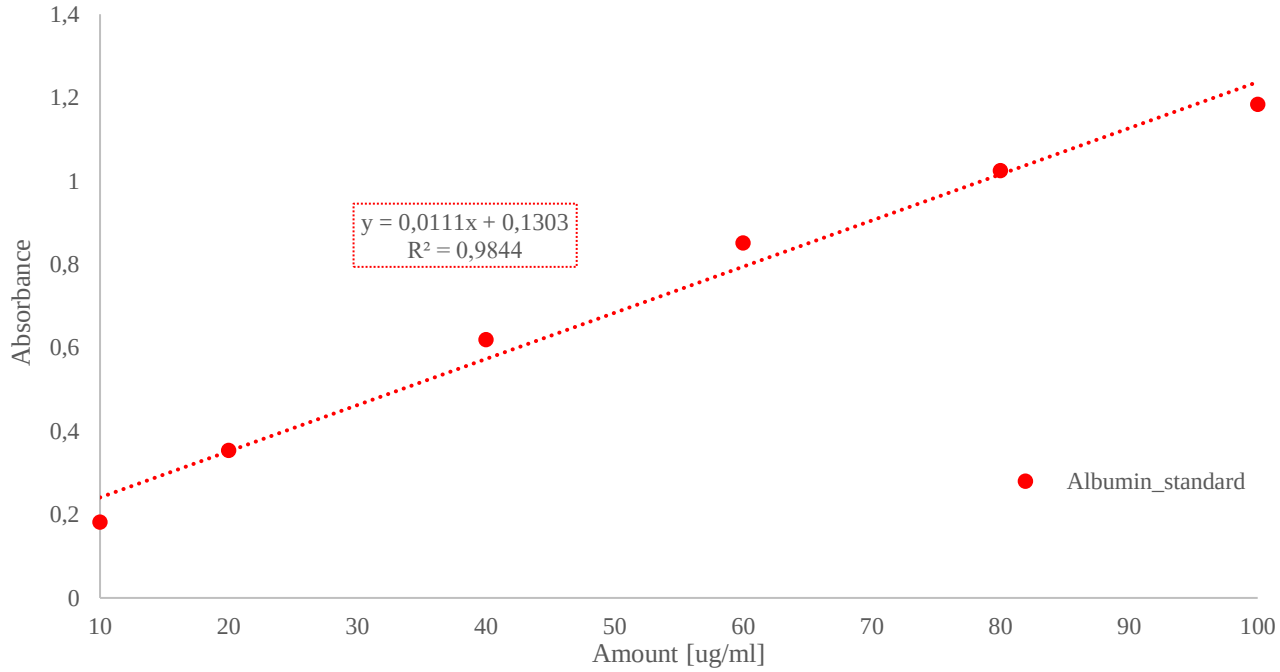

Fig. 44: Calibration curve measured for stable Fibroblast growth factor 2 using albumin standard at a given concentration for middle concentrations (10–100 µg/ml) measured by UV-VIS spectrophotometer at 595 nm in the presence of Bradford reagent.

5.2.5 Monitoring of model proteins release using inserts (Method B)

Because of the high cost of stable fibroblast growth factor, model proteins were used for the first control insert measurements. Two model proteins were selected, namely human lysozyme (14.7 kg.mol^{-1}) and human albumin (69 kg.mol^{-1}). Lysozyme has a lower molecular weight and albumin larger than FGF2-stab. The difference was also the continuous measurement when PBS was always removed from the bottom tray and replaced with an equal volume of pure buffer.

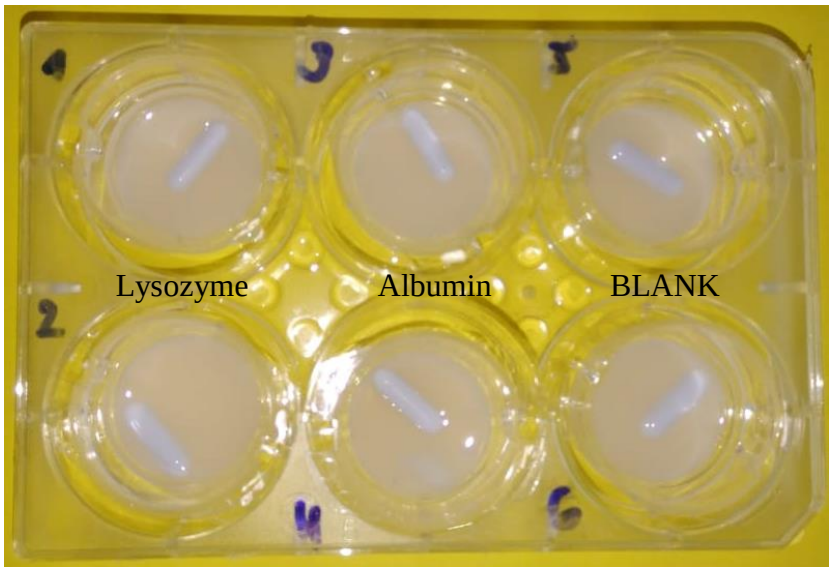

Fig. 45 : Sample distribution in insert for first control measurement using model proteins.

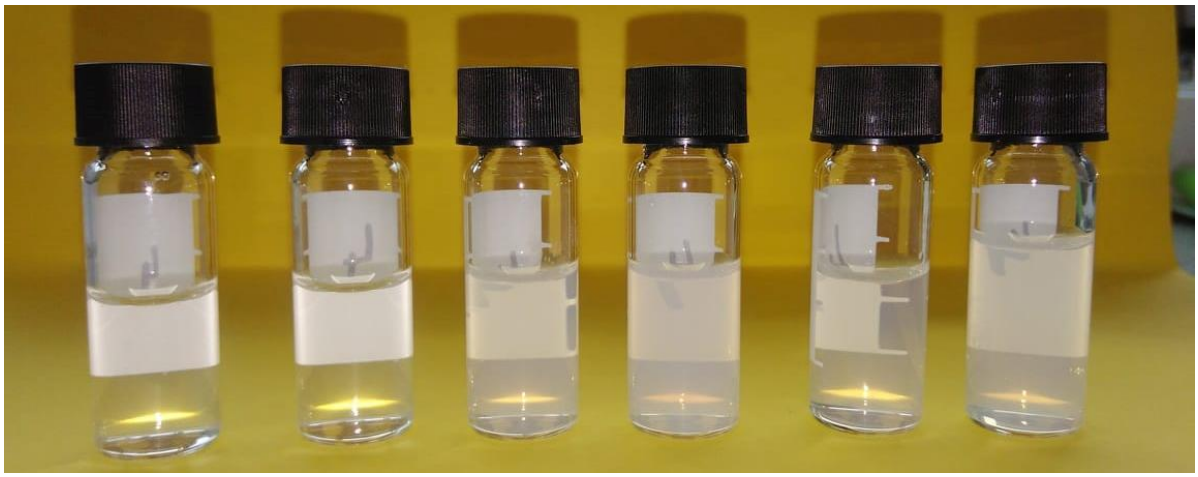

Fig. 46: Albumin samples taken at 2, 3, 9, 16, 17, and 22 days where there is a slight turbidity of the disintegrating gel, but it is not as large as samples measured by method A.

For the Measurement I by method B, one insert (see Fig. 45) was prepared, containing two samples of lysozyme, albumin and BLANK. The measurements lasted for 22 days, samples were taken at 1, 2, 3, 9, 16, 17 and 22 days and the results are recorded as green curves in the graphs (see Fig. 47,Fig. 48). For both types of proteins, there is a rapid release of approximately one-third of the incorporated amount within 3 days. For lysozyme, this amount is about 7% higher due to lower molecular weight and thus easier release from the thermosensitive ABA hydrogel than for albumin. In the range of 3-17 days (lysozyme) and 3-22 days (albumin), no release was measured by UV-VIS spectrophotometry. A sample of lysozyme collected after 22 days released approximately 20% of the protein mixed into ABA hydrogel. Because of this release, a two-step release of both lysozyme and albumin was envisaged for longer measurements. The total amount of lysozyme released in 22 days was 57% and of albumin was 32%.

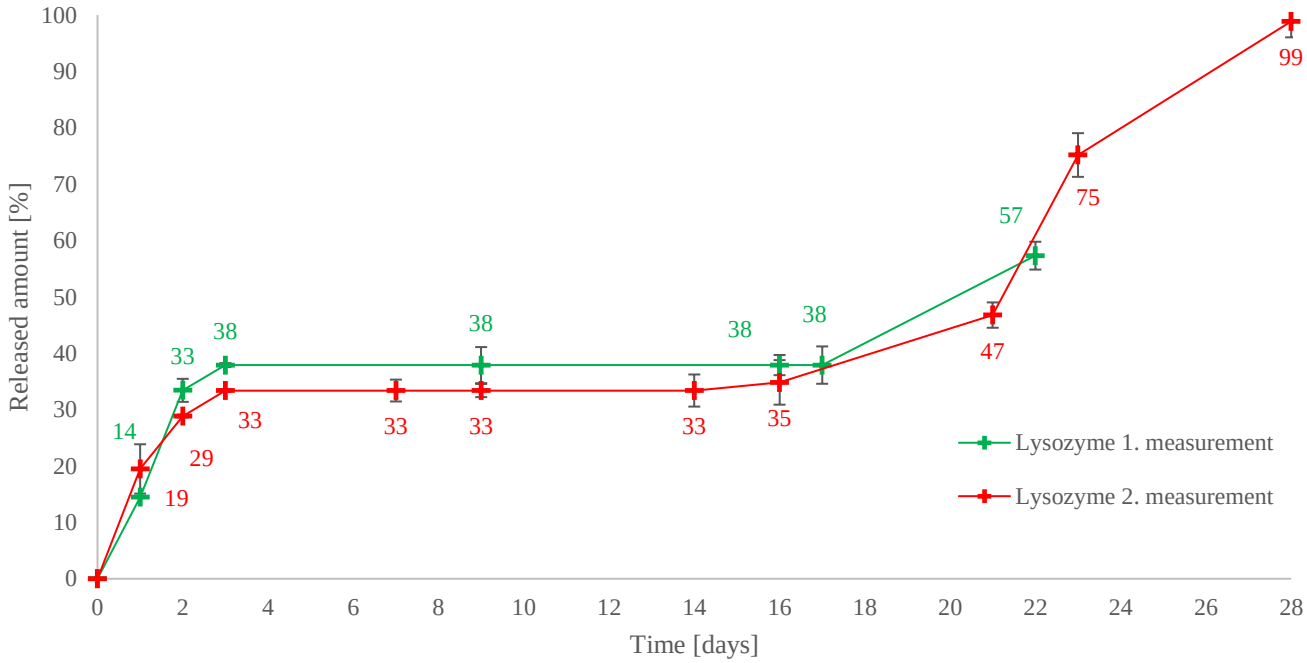

Fig. 47: Graph of lysozyme release from thermosensitive ABA hydrogel. Two-step release is evident, and all measurements were made with UV-VIS spectrophotometer in the presence of Bradford reagent.

For the repeated measurement II by method B of modular proteins, 2 inserts were prepared, each contained 5 samples of a model protein (lysozyme, albumin) and one BLANK. PBS collection from the trays was performed at 1, 2, 3, 7, 9, 14, 16, 21, 23 and 28 days. The results are shown as red curves in the graphs (see Fig. 47Fig. 48). As shown in the graphs, two-step release was observed as was expected in the previous measurement.

Comparing both the lysozyme and albumin curves of I. and II. measurements, it was evident that the release of proteins up to 22 days was comparable, and by increasing the measurement time (to 28 days), 99% of the lysozyme and 75% of the albumin were released. Due to the degradation of ABA hydrogel and hence the loss of mechanical properties (see Fig. 49), the release time was no longer prolonged, and 28 days was the maximum time.

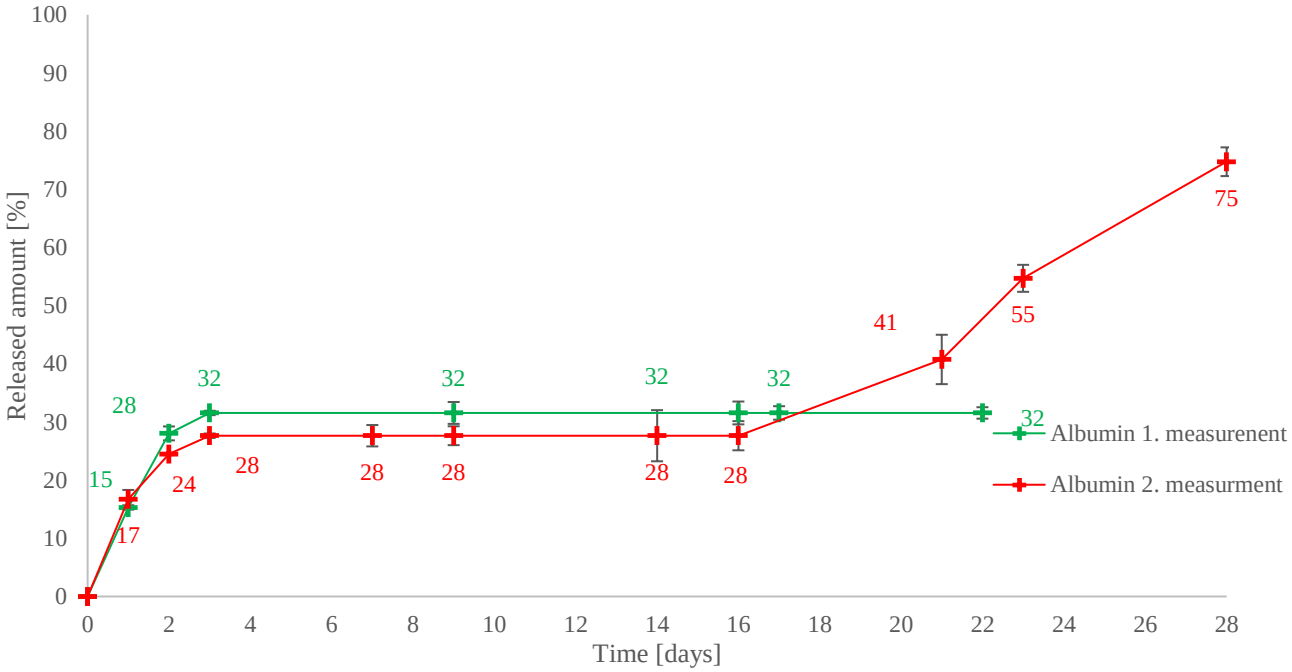

Fig. 48: Graph of Albumin release from thermosensitive ABA hydrogel. Two-step release is evident, and all measurements were made with UV-VIS spectrophotometer in the presence of Bradford reagent.

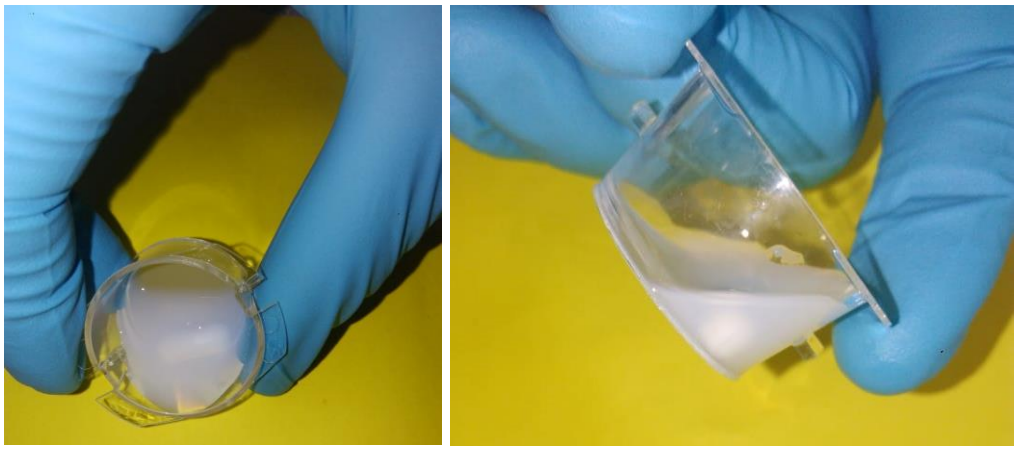

Fig. 49: Figures showing degraded PLGA-PEG-PLGA hydrogel after 28 days.

The difference in the released amount of model proteins (lysozyme, albumin) was given by different molecular weight and mainly by the polarity rate. This also explained the two-step release of proteins. Since both proteins had polar and non-polar residues on the surface of the molecule, it was differently bound to the hydrogel micelles (see Fig. 50). Lysozyme had more polar groups on the surface, and more protein was probably bound to the micelle surface, and only part of it was in its centre. Thus, a higher total amount of mixed protein was released. In contrast, albumin on the surface was more non-polar, it had 11 hydrophobic binding sites and was thus more bound to the centre of the micelle and only a portion remained on the surface. This resulted in the release of less protein than lysozyme. Hence, the two-step release was due

to the initial release of the proteins bound to the micelle shell. The second stage occurred at a time when ABA hydrogel was gradually degraded and proteins bound to the micelle centre were released. In our case, the second release level was recorded from approximately 14 days of measurement.

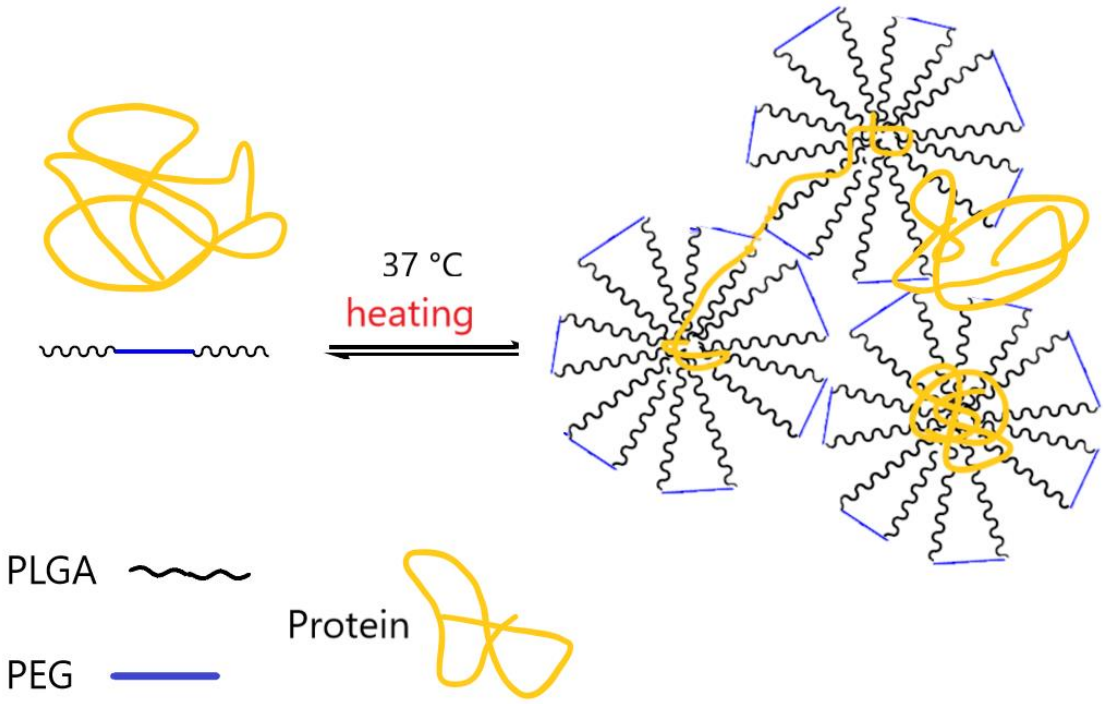

Fig. 50: Model depicting the possibility of protein binding to micelles of PLGA-PEG-PLGA hydrogel as a function of protein polarity.

5.2.6 Method B of measurement of stable Fibroblast growth factor 2 (FGF2-stab) release using inserts (Measurement III.)

The release of stable fibroblast growth factor was measured by UV-VIS spectrophotometer at 595 nm in the presence of Bradford reagent using inserts. The preparation and measurement of the samples were the same as for the model proteins. The released amount of FGF2-stab was measured after 1, 2, 3, 7, 9, 14, 16, 21 and 23 days. The release results of four FGF2-stab samples were recorded in the graph (see Fig. 51).

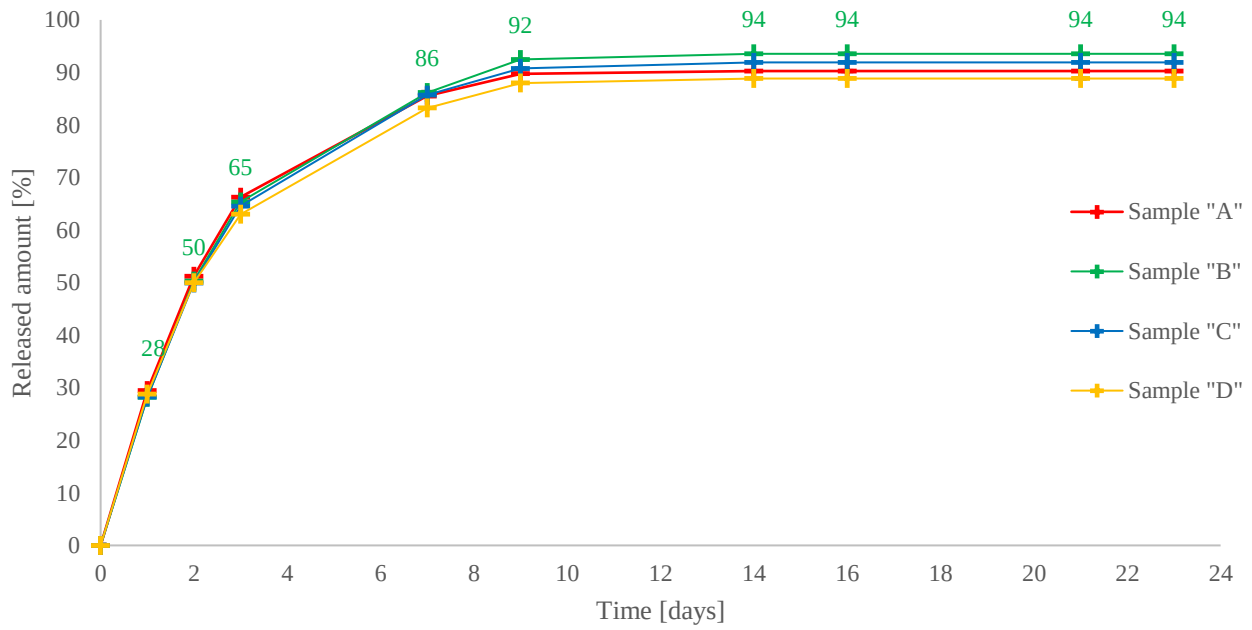

Fig. 51: Comparison of four samples of the released amount of FGF2-stab from PLGA-PEG-PLGA hydrogel using inserts and measured by UV-VIS spectrophotometer at 595 nm using Bradford reagent.

When comparing the results, it was evident that for all FGF2-stab samples there was one-step release from the PLGA-PEG-PLGA carrier. During day 1, approximately 28% of the incorporated FGF2-stab was released. The maximum amount of all samples was measured after 14 days and was approximately 94% of total incorporated FGF2-stab (Fig. 51). The well-controlled one-step release was due to the type of binding of FGF2-stab to the PLGA-PEG-PLGA gel. Since FGF2-stab was polar on the surface and thus hydrophilic due to the presence of Arg, Cys and Ser residues, most of the FGF2-stabs were bound to the micelle shell present in the gel. FGF2-stab was released by the first order of non-Fickian diffusion, which is time and diffusion depended of FGF2-stab but not reflected the erosion and degradation of the PLGA-PEG-PLGA hydrogel. First order diffusion was verified by calculation using the equation:

$$-\frac{dc}{dt} = k \cdot c, \tag{1}$$

when k= 0,423 for sample “A”. For a longer release time of FGF2-stab from the gel, modification of the PLGA-PEG-PLGA copolymer with itaconic acid (according to our previous work [21]) can be used. This modification gives COOH groups to ironically bond FGF2-stab to the gel and thus slow-down its release.

6 CONCLUSION

The aim of this diploma thesis was to ensure reproducible detection of released healing proteins from thermosensitive polymer carriers. UV-VIS spectrophotometry at 595 nm was used as a method for analysing the amount released. Bradford reagent was used because it interacts with proteins and shifts their absorption maxima from 280 nm to 595 nm. Another method used was SDS-page electrophoresis, which divides molecules by molecular weight.

In method A of measurement, stable fibroblast growth factor 2 (FGF2-stab) was released from the amphiphilic thermosensitive PLGA-PEG-PLGA hydrogel that forms the gel at physiological temperature. The FGF2-stab was mixed into the copolymer solution and allowed to the gel in an incubator at 37 °C. A phosphate buffer into which FGF2-stab was released was dosed above the gel. The problem was the gel disintegration, which influenced the UV-VIS spectrophotometer measurement and the results were distorted. At this measurement stage, the maximum release amount was about 35% in 72 hours.

The inserts consisting of two trays were the solution of the affected measurement by degrading gel. One smaller that had a membrane at the bottom and into which the PLGA-PEG-PLGA gel with the protein was dosed and the other larger to which phosphate buffer was dosed and into which the protein was released through the membrane. Model proteins, lysozyme and albumin, were firstly used to set-up the method instead of expensive FGF2-stab. For these proteins, two-step release from the PLGA-PEG-PLGA hydrogel was observed. The two-step release was due to polarity when lysozyme and albumin showing both polar and surface non-polar character. Since PLGA-PEG-PLGA is an amphiphilic hydrogel and forms micelles, a portion of the proteins was bound to the micelle surface and part of the proteins into their nuclei. In the first step, the proteins bound to the surface were released and in the second step (when the gel began to degrade) the proteins bound to the micelle core were released. Aproximately 40% of lysozyme was released in the first step and almost 100% in the second step. As for albumin, about 30% was released in the first step and 75% in the second step probably due to the slower diffusion because of higher molecular weight (69 $kg.mol^{-1}$) in comparison to lysozyme (14.7 $kg.mol^{-1}$).

Finally, inserts were used to measure the release of anionic surface charged polar FGF2-stab (25 $kg.mol^{-1}$) from the PLGA-PEG-PLGA hydrogel. Contrary to albumin a lysozyme, one-step well-controlled first-order release was observed. Within 14 days, approximately 95% of the total amount of protein incorporated in polymer hydrogel was released proving the thermosensitive hydrogel to be an ideal FGF2-stab carrier suitable for biomedical applications.

Due to the high FGF2-stab hydrolytic stability (approx. 20 days at 37 °C) the release time can be even prolonged by a simple modification of PLGA-PEG-PLGA with COOH groups that will physically bind FGF2-stab tightly to the hydrogel and slow down its diffusion up to 21 days corresponding to hydrogel degradation.

7 REFERENCES

[1] MURRAY, Robert K. *Harperova Biochemie*. 4. Jinočany: H+H, 2002. Lange medical book. ISBN 80-731-9013-3.

[2] PETERS, Theodore. *All about albumin: biochemistry, genetics, and medical applications*. San Diego: Academic Press, c1996. ISBN 01-255-2110-3.

[3] LARSEN, Maja Thim, Matthias KUHLMANN, Michael Lykke HVAM a Kenneth A. HOWARD. Albumin-based drug delivery: harnessing nature to cure disease. *Molecular and Cellular Therapies*. 2016, **4**(1). DOI: 10.1186/s40591-016-0048-8. ISSN 2052-8426. Dostupné také z: http://molcelltherapies.com/article/view/25

[4] KRATZ, Felix. Albumin as a drug carrier: Design of prodrugs, drug conjugates and nanoparticles. *Journal of Controlled Release*. 2008, **132**(3), 171-183. DOI: 10.1016/j.jconrel.2008.05.010. ISSN 01683659. Dostupné také z: https://linkinghub.elsevier.com/retrieve/pii/S0168365908002551

[5] HE, Xiao Min a Daniel C. CARTER. Atomic structure and chemistry of human serum albumin. *Nature*. 1992, **358**(6383), 209-215. DOI: 10.1038/358209a0. ISSN 0028-0836. Dostupné také z: http://www.nature.com/articles/358209a0

[6] DING, Dan a Xiqun JIANG. Drug Delivery from Protein-Based Nanoparticles. *Bioinspired and Biomimetic Polymer Systems for Drug and Gene Delivery*. Weinheim, Germany, 2014, 2014-12-19, , 149-170. DOI: 10.1002/9783527672752.ch6. ISBN 9783527672752. Dostupné také z: http://doi.wiley.com/10.1002/9783527672752.ch6

[7] C. LIEBLER, Daniel. Introduction to proteomics: tools for the new biology. Totowa, N.J: Humana, 2002. ISBN 978-089-6039-919

[8] BÁRTA, Jan, Veronika BÁRTOVÁ a Vladislav ČURN. Analýza proteinů pomocí automatické čipové elektroforézy Experion a porovnání s metodou SDS-PAGE. Chemické listy. 2010, 104(01), 33-40. ISSN 1213-7103. Dostupné také z: http://www.chemicke-listy.cz/docs/full/2010_01_33-40.pdf

[9] YUN, Ye-Rang, Jong Eun WON, Eunyi JEON, et al. Fibroblast Growth Factors: Biology, Function, and Application for Tissue Regeneration. *Journal of Tissue Engineering*. 2010, **1**(1). DOI: 10.4061/2010/218142. ISSN 2041-7314. Dostupné také z: http://journals.sagepub.com/doi/10.4061/2010/218142

[10] BARRIENTOS, Stephan, Olivera STOJADINOVIC, Michael S. GOLINKO, Harold BREM a Marjana TOMIC-CANIC. PERSPECTIVE ARTICLE: Growth factors and cytokines in wound healing. *Wound Repair and Regeneration*. 2008, **16**(5), 585-601.

DOI: 10.1111/j.1524-475X.2008.00410.x. ISSN 10671927. Dostupné také z: http://doi.wiley.com/10.1111/j.1524-475X.2008.00410.x

[11] NUGENT, Matthew A a Renato V IOZZO. Fibroblast growth factor-2. *The International Journal of Biochemistry & Cell Biology*. 2000, **32**(2), 115-120. DOI: 10.1016/S1357-2725(99)00123-5. ISSN 13572725. Dostupné také z: http://linkinghub.elsevier.com/retrieve/pii/S1357272599001235

[12] DOSTÁL, Jiří. *Lékařská chemie II: bioorganická chemie*. 3. vyd. Brno: Masarykova univerzita, 2011. ISBN 978-80-210-5538-4.

[13] VOET, Donald a Judith G. VOET. *Biochemie*. Praha: Victoria Publishing, 1995. ISBN 80-856-0544-9.

[14] STAPLETON, A., M. R. NOOR, J. SWEENEY, et al. The direct piezoelectric effect in the globular protein lysozyme. *Applied Physics Letters*. 2017, **111**(14). DOI: 10.1063/1.4997446. ISSN 0003-6951. Dostupné také z: http://aip.scitation.org/doi/10.1063/1.4997446

[15] CALLEWAERT, Lien a Chris W. MICHIELS. Lysozymes in the animal kingdom. *Journal of Biosciences*. 2010, **35**(1), 127-160. DOI: 10.1007/s12038-010-0015-5. ISSN 0250-5991. Dostupné také z: http://link.springer.com/10.1007/s12038-010-0015-5

[16] MAGA, ELIZABETH A., GARY B. ANDERSON, JAMES S. CULLOR, WAYNE SMITH a JAMES D. MURRAY. Antimicrobial Properties of Human Lysozyme Transgenic Mouse Milk. *Journal of Food Protection*. 1998, **61**(1), 52-56. DOI: 10.4315/0362-028X-61.1.52. ISSN 0362-028X. Dostupné také z: http://jfoodprotection.org/doi/abs/10.4315/0362-028X-61.1.52

[17] HOARE, Todd R. a Daniel S. KOHANE. Hydrogels in drug delivery: Progress and challenges. *Polymer*. 2008, **49**(8), 1993-2007. DOI: 10.1016/j.polymer.2008.01.027. ISSN 00323861. Dostupné také z: https://linkinghub.elsevier.com/retrieve/pii/S0032386108000487

[18] LI, Jianyu a David J. MOONEY. Designing hydrogels for controlled drug delivery. *Nature Reviews Materials*. 2016, **1**(12). DOI: 10.1038/natrevmats.2016.71. ISSN 2058-8437. Dostupné také z: http://www.nature.com/articles/natrevmats201671

[19] ELSTAD, Nancy L. a Kirk D. FOWERS. OncoGel (ReGel/paclitaxel) — Clinical applications for a novel paclitaxel delivery system. *Advanced Drug Delivery Reviews*. 2009, **61**(10), 785-794. DOI: 10.1016/j.addr.2009.04.010. ISSN 0169409X. Dostupné také z: https://linkinghub.elsevier.com/retrieve/pii/S0169409X09001422

[20] SAMLOWSKI, Wolfram E., John R. MCGREGOR, Maria JUREK, Miroslav BAUDYS, Gaylen M. ZENTNER a Kirk D. FOWERS. ReGel ® Polymer-based

Delivery of Interleukin-2 as a Cancer Treatment. *Journal of Immunotherapy*. 2006, **29**(5), 524-535. DOI: 10.1097/01.cji.0000211306.05869.25. ISSN 1524-9557. Dostupné také z: https://insights.ovid.com/crossref?an=00002371-200609000-00007

[21] MICHLOVSKÁ, Lenka, Lucy VOJTOVÁ, Ludmila MRAVCOVÁ, Soňa HERMANOVÁ, Jiří KUČERÍK a Josef JANČÁŘ. Functionalization Conditions of PLGA-PEG-PLGA Copolymer with Itaconic Anhydride. *Macromolecular Symposia*. 2010, **295**(1), 119-124. DOI: 10.1002/masy.200900071. ISSN 10221360. Dostupné také z: http://doi.wiley.com/10.1002/masy.200900071

[22] MURRAY, Robert K. *Harperova Biochemie*. Jinočany, 2002. Lange medical book. ISBN 80-731-9013-3.

[23] Paclitaxel. *Drugs* [online]. [cit. 2019-03-23]. Dostupné z: https://www.drugs.com/mtm/paclitaxel.html

[24] MICHLOVSKÁ, L., L. VOJTOVÁ, O. HUMPA, J. KUČERÍK, J. ŽÍDEK a J. JANČÁŘ. Hydrolytic stability of end-linked hydrogels from PLGA–PEG–PLGA macromonomers terminated by α,ω-itaconyl groups. *RSC Advances*. 2016, **6**(20), 16808-16816. DOI: 10.1039/C5RA26222D. ISSN 2046-2069. Dostupné také z: http://xlink.rsc.org/?DOI=C5RA26222D

[25] SANTANDER-ORTEGA, M.J., A.B. JÓDAR-REYES, N. CSABA, D. BASTOS-GONZÁLEZ a J.L. ORTEGA-VINUESA. Colloidal stability of Pluronic F68-coated PLGA nanoparticles: A variety of stabilisation mechanisms. *Journal of Colloid and Interface Science*. 2006, **302**(2), 522-529. DOI: 10.1016/j.jcis.2006.07.031. ISSN 00219797. Dostupné také z: https://linkinghub.elsevier.com/retrieve/pii/S0021979706005947

[26] SHIRWAIKER, R.A., M.F. PURSER a R.A. WYSK. Scaffolding hydrogels for rapid prototyping based tissue engineering. *Rapid Prototyping of Biomaterials*. Elsevier, 2014, 2014, , 176-200. DOI: 10.1533/9780857097217.176. ISBN 9780857095992. Dostupné také z: https://linkinghub.elsevier.com/retrieve/pii/B9780857095992500064

[27] BEARAT, H.H. a B.L. VERNON. Environmentally responsive injectable materials. *Injectable Biomaterials*. Elsevier, 2011, 2011, , 263-297. DOI: 10.1533/9780857091376.3.263. ISBN 9781845695880. Dostupné také z: https://linkinghub.elsevier.com/retrieve/pii/B9781845695880500115

[28] SCHMALJOHANN, D. Thermo- and pH-responsive polymers in drug delivery☆. *Advanced Drug Delivery Reviews*. 2006, **58**(15), 1655-1670. DOI: 10.1016/j.addr.2006.09.020. ISSN 0169409X. Dostupné také z: https://linkinghub.elsevier.com/retrieve/pii/S0169409X06001839

[29] PRIYA JAMES, Honey, Rijo JOHN, Anju ALEX a K.R. ANOOP. Smart polymers for the controlled delivery of drugs – a concise overview. *Acta Pharmaceutica Sinica*

B. 2014, **4**(2), 120-127. DOI: 10.1016/j.apsb.2014.02.005. ISSN 22113835. Dostupné také z: https://linkinghub.elsevier.com/retrieve/pii/S2211383514000252

[30] QIU, Yong a Kinam PARK. Environment-sensitive hydrogels for drug delivery. *Advanced Drug Delivery Reviews*. 2001, **53**(3), 321-339. DOI: 10.1016/S0169-409X(01)00203-4. ISSN 0169409X. Dostupné také z: http://linkinghub.elsevier.com/retrieve/pii/S0169409X01002034

[31] CHO, Hyunah, Jieming GAO a Glen S. KWON. PEG- b -PLA micelles and PLGA- b -PEG- b -PLGA sol–gels for drug delivery. *Journal of Controlled Release*. 2016, **240**, 191-201. DOI: 10.1016/j.jconrel.2015.12.015. ISSN 01683659. Dostupné také z: https://linkinghub.elsevier.com/retrieve/pii/S0168365915302674

[32] SONG, Zhimei, Runliang FENG, Min SUN, Chenyu GUO, Yan GAO, Lingbing LI a Guangxi ZHAI. Curcumin-loaded PLGA-PEG-PLGA triblock copolymeric micelles: Preparation, pharmacokinetics and distribution in vivo. *Journal of Colloid and Interface Science*. 2011, **354**(1), 116-123. DOI: 10.1016/j.jcis.2010.10.024. ISSN 00219797. Dostupné také z: https://linkinghub.elsevier.com/retrieve/pii/S0021979710011938

[33] MIYAZAKI, Makoto, Tomoki MAEDA, Kenji HIRASHIMA, Naruki KUROKAWA, Koji NAGAHAMA a Atsushi HOTTA. PEG-based nanocomposite hydrogel: Thermoresponsive sol-gel transition controlled by PLGA-PEG-PLGA molecular weight and solute concentration. *Polymer*. 2017, **115**, 246-254. DOI: 10.1016/j.polymer.2017.03.016. ISSN 00323861. Dostupné také z: https://linkinghub.elsevier.com/retrieve/pii/S003238611730263X

[34] WEI, Hua, Si-Xue CHENG, Xian-Zheng ZHANG a Ren-Xi ZHUO. Thermo-sensitive polymeric micelles based on poly(N-isopropylacrylamide) as drug carriers. *Progress in Polymer Science*. 2009, **34**(9), 893-910. DOI: 10.1016/j.progpolymsci.2009.05.002. ISSN 00796700. Dostupné také z: https://linkinghub.elsevier.com/retrieve/pii/S0079670009000525

[35] GANDHI, Arijit, Abhijit PAUL, Suma Oommen SEN a Kalyan Kumar SEN. Studies on thermoresponsive polymers: Phase behaviour, drug delivery and biomedical applications. *Asian Journal of Pharmaceutical Sciences*. 2015, **10**(2), 99-107. DOI: 10.1016/j.ajps.2014.08.010. ISSN 18180876. Dostupné také z: https://linkinghub.elsevier.com/retrieve/pii/S1818087614000634

[36] VYAS, Bijal, Sadafara PILLAI, Anita BAHADUR a Pratap BAHADUR. A Comparative Study on Micellar and Solubilizing Behavior of Three EO-PO Based Star Block Copolymers Varying in Hydrophobicity and Their Application for the In Vitro Release of Anticancer Drugs. *Polymers*. 2018, **10**(1). DOI: 10.3390/polym10010076. ISSN 2073-4360. Dostupné také z: http://www.mdpi.com/2073-4360/10/1/76

[37] MOHAMMED, Marwah N., Kamal Bin YUSOH a Jun Haslinda Binti Haji SHARIFFUDDIN. Poly(N-vinyl caprolactam) thermoresponsive polymer in novel drug delivery systems: A review. *Materials Express*. 2018, **8**(1), 21-34. DOI: 10.1166/mex.2018.1406. ISSN 2158-5849. Dostupné také z: http://www.ingentaconnect.com/content/10.1166/mex.2018.1406

[38] DENG, Hongzhang, Anjie DONG, Jibin SONG a Xiaoyuan CHEN. Injectable thermosensitive hydrogel systems based on functional PEG/PCL block polymer for local drug delivery. *Journal of Controlled Release*. 2019, **297**, 60-70. DOI: 10.1016/j.jconrel.2019.01.026. ISSN 01683659. Dostupné také z: https://linkinghub.elsevier.com/retrieve/pii/S0168365919300537

[39] LIECHTY, William B., David R. KRYSCIO, Brandon V. SLAUGHTER a Nicholas A. PEPPAS. Polymers for Drug Delivery Systems. *Annual Review of Chemical and Biomolecular Engineering*. 2010, **1**(1), 149-173. DOI: 10.1146/annurev-chembioeng-073009-100847. ISSN 1947-5438. Dostupné také z: http://www.annualreviews.org/doi/10.1146/annurev-chembioeng-073009-100847

[40] KIKUCHI, Akihiko a Teruo OKANO. Pulsatile drug release control using hydrogels. *Advanced Drug Delivery Reviews*. 2002, **54**(1), 53-77. DOI: 10.1016/S0169-409X(01)00243-5. ISSN 0169409X. Dostupné také z: http://linkinghub.elsevier.com/retrieve/pii/S0169409X01002435

[41] HUANG, Xiao a Christopher S BRAZEL. On the importance and mechanisms of burst release in matrix-controlled drug delivery systems. *Journal of Controlled Release*. 2001, **73**(2-3), 121-136. DOI: 10.1016/S0168-3659(01)00248-6. ISSN 01683659. Dostupné také z: http://linkinghub.elsevier.com/retrieve/pii/S0168365901002486

[42] PATEL, Jayvadan a Anita PATEL. Artificial Neural Networking in Controlled Drug Delivery. *Artificial Neural Network for Drug Design, Delivery and Disposition*. Elsevier, 2016, 2016, , 195-218. DOI: 10.1016/B978-0-12-801559-9.00010-7. ISBN 9780128015599. Dostupné také z: https://linkinghub.elsevier.com/retrieve/pii/B9780128015599000107

[43] Rabišková CSc, M. AND Fričová, V. Perorální formy s řízeným uvolňováním léčiv. Solen, 2008/11/01 2008, vol. 4, no. 4, p. 186-190.

[44] ELVIRA, C., A. GALLARDO, J. ROMAN a A. CIFUENTES. Covalent Polymer-Drug Conjugates. *Molecules*. 2005, **10**(1), 114-125. DOI: 10.3390/10010114. ISSN 1420-3049. Dostupné také z: http://www.mdpi.com/1420-3049/10/1/114

[45] SNEHA, P. a C. GEORGE PRIYA DOSS. Molecular Dynamics. *Personalized Medicine*. Elsevier, 2016, 2016, **2016**(102), 181-224. Advances in Protein Chemistry

and Structural Biology. DOI: 10.1016/bs.apcsb.2015.09.004. ISBN 9780128047958. Dostupné také z: https://linkinghub.elsevier.com/retrieve/pii/S187616231500067X

[46] QUEIROZ, J.A., C.T. TOMAZ a J.M.S. CABRAL. Hydrophobic interaction chromatography of proteins. *Journal of Biotechnology*. 2001, **87**(2), 143-159. DOI: 10.1016/S0168-1656(01)00237-1. ISSN 01681656. Dostupné také z: http://linkinghub.elsevier.com/retrieve/pii/S0168165601002371

[47] DVORAK, Pavel, David BEDNAR, Pavel VANACEK, et al. Computer-assisted engineering of hyperstable fibroblast growth factor 2. *Biotechnology and Bioengineering*. 2018, **115**(4), 850-862. DOI: 10.1002/bit.26531. ISSN 00063592. Dostupné také z: http://doi.wiley.com/10.1002/bit.26531

[48] MICHLOVSKÁ, Lenka. *Synthesis and characterization of multifunctionalized biodegradable copolymers*. Brno, 2014. Doctoral thesis. Vysoké učení technické, Fakulta chemická.

[49] OBORNÁ, Jana. *Řízené uvolňování léčiv z biodegradabilních hydrogelů*. Brno, 2018. Dizertační práce. Vysoké učení technické, Fakulta chemická. Vedoucí práce Prof. RNDr. Milada Vávrová, CSc.

[50] MICHLOVSKÁ, L., L. VOJTOVÁ, O. HUMPA, J. KUČERÍK, J. ŽÍDEK and J. JANČÁŘ. Hydrolytic stability of end-linked hydrogels from PLGA–PEG–PLGA macromonomers terminated by α,ω-itaconyl groups. RSC Advances. 2016, 6(20), 16808-16816. DOI: 10.1039/C5RA26222D. ISSN 2046-2069. Available from: http://xlink.rsc.org/?DOI=C5RA26222D

[51] WILSON, C.R., J.K. BUTZ a M.C. MENGEL. Methods for Analysis of Gastrointestinal Toxicants☆. *Reference Module in Biomedical Sciences*. Elsevier, 2014, 2014. DOI: 10.1016/B978-0-12-801238-3.02125-5. ISBN 9780128012383. Dostupné také z: https://linkinghub.elsevier.com/retrieve/pii/B9780128012383021255

[52] HACKNEY, Anthony C. Athlete Testing, Analytical Procedures, and Adverse Analytical Findings. *Doping, Performance Enhancing Drugs, and Hormones in Sport*. Elsevier, 2018, 2018, , 113-127. DOI: 10.1016/B978-0-12-813442-9.00010-9. ISBN 9780128134429. Dostupné také z: https://linkinghub.elsevier.com/retrieve/pii/B9780128134429000109

[53] RAO, Zi-Kun, Rui CHEN, Hong-Yu ZHU, Yang LI, Yu LIU a Jian-Yuan HAO. Carboxylic Terminated Thermo-Responsive Copolymer Hydrogel and Improvement in Peptide Release Profile. *Materials*. 2018, **11**(3). DOI: 10.3390/ma11030338. ISSN 1996-1944. Dostupné také z: http://www.mdpi.com/1996-1944/11/3/338

[54] TRAN, Van-Thanh, Jean-Pierre KARAM, Xavier GARRIC, Jean COUDANE, Jean-Pierre BENOÎT, Claudia N. MONTERO-MENEI a Marie-Claire VENIER-

JULIENNE. Protein-loaded PLGA–PEG–PLGA microspheres: A tool for cell therapy. *European Journal of Pharmaceutical Sciences*. 2012, **45**(1-2), 128-137. DOI: 10.1016/j.ejps.2011.10.030. ISSN 09280987. Dostupné také z: https://linkinghub.elsevier.com/retrieve/pii/S0928098711003903

[55] MILACIC, Vesna a Steven P. SCHWENDEMAN. Lysozyme Release and Polymer Erosion Behavior of Injectable Implants Prepared from PLGA-PEG Block Copolymers and PLGA/PLGA-PEG Blends. *Pharmaceutical Research*. 2014, **31**(2), 436-448. DOI: 10.1007/s11095-013-1173-6. ISSN 0724-8741. Dostupné také z: http://link.springer.com/10.1007/s11095-013-1173-6

[56] QIAO, Mingxi, Dawei CHEN, Xichen MA a Yanjun LIU. : Synthesis and effect of copolymer composition on the drug release from the copolymer-based hydrogels. *International Journal of Pharmaceutics*. 2005, **294**(1-2). DOI: 10.1016/j.ijpharm.2005.01.017. ISSN 03785173. Dostupné také z: https://linkinghub.elsevier.com/retrieve/pii/S0378517305000840

8 LIST OF SYMBOLS

ABA	PLGA-PEG-PLGA copolymer
Ala	Alanine
Arg	Arginine
Asn	Asparagine
Asp	Aspartic acid
bFGF	basic Fibroblast growth factor
BSA	Bovine serum albumin
$CDCl_3$	Denatured chloroform
COOH	Carboxyl group
FGF	Fibroblast growth factor
FGFR	Fibroblast growth factor receptors
GEWL	Goose´s lysozyme
G´	Storage modulus
G´´	Loss modulus
Glu	Glutamic acid
Gly	Glycine
GPC	Gel permeation chromatography
HEWL	Hen´s lysozyme
HSA	Human serum albumin
Ile	Isoleucine
LCST	Low critical solution temperature
LGTT	Lower gel transition temperature
MAP	mitogen-activated protein
Mn	Number average molecular weight
Mw	Weight average molecular weight
NAG	N-acetylglukosamine
NAM	N-acetylmuamic acid
NMR	Nuclear magnetic resonance
PBS	Phosphate buffer saline
PCL	Poly (caprolactone)
PDI	Polydispersity
PEG	Poly (ethyleneglycole)
PEO	Poly (ethylene oxide)

PLGA	Poly (lactide-co-glycolide acid)
PNIPAAm	Poly (N-isopropylacrylamide)
PNVCL	Poly (N-vinylcaprolactam)
PPO	Poly (propylene oxide)
PS	Polystyrene
ROP	Ring opening polymerization
RT	Room temperature
SDS	Sodium dodecylsulphate
SEC	Size-exclusion chromatography
Ser	Serine
THF	Tetrahydrofuran
TMS	Tetramethylsilane
Trp	Tryptophan
UCST	Upper critical solution temperature
UGTT	Upper gel transition temperature
UV	Ultraviolet radiation
VEGF	Vascular endothelial growth factor
VIS	Visible radiation

9 LIST OF TABLES

10 LIST OF FIGURES